# Task Modeling: Approximating Multitask Predictions for Cross-Task Transfer

Anonymous submission

## Abstract

We study the problem of learning a target task when data samples from several auxiliary source tasks are available. Examples of this problem appear in multitask learning, where several tasks are combined jointly, and weak supervision, where multiple programmatic labels are generated for each sample. Because of task data's heterogeneity, negative interference is a critical challenge for solving this problem. Previous works have measured first-order task affinity as an effective metric, yet it becomes less accurate for approximating higher-order transfers. We propose a procedure called task modeling to model first- and higher-order transfers. This procedure samples subsets of source tasks and estimates surrogate functions to approximate multitask predictions. We show theoretical and empirical results that task models can be estimated in nearly-linear time in the number of tasks and accurately approximate multitask predictions. Thus, the target task's performance can be optimized using task models to select source tasks. We validate this approach on various datasets and performance metrics. Our method increases accuracy up to 3.6% over existing methods on five text classification tasks with noisy supervision sources. Additionally, task modeling can be applied to group robustness and fairness metrics. Ablation studies show that task models can accurately predict whether or not a set of up to four source tasks transfer positively to the target task.

## 1 Introduction

Given a set of $k$ auxiliary source tasks and a primary target task of interest, how can we select the beneficial ones for the target task? This question is motivated by a number of applications. In multitask learning [6, 10, 13], several tasks are learned simultaneously. The learned model can be further fine-tuned for a single task [29]. Depending on task relatedness, multitask learning may worsen performance compared to single task learning [7], a phenomenon known as negative transfer [26, 31]. Another example is weak supervision [33, 35]: each sample is annotated with multiple (possibly conflicting) labels, generated by labeling functions specified with domain knowledge. The labeling functions can be viewed as source tasks alongside the target task in a multitask model [34].

Early work shows that information sharing across tasks can be realized with explicit regularization in shallow linear and kernel models [1, 17, 58]. With deep neural networks, sharing information across tasks is more challenging [52]. A naive solution for finding the most beneficial source tasks is to search through all possible combinations of source tasks. However, this is prohibitively expensive as $k$ grows. Another solution is to determine first-order task affinity by training one model for every source-target pair [42]. Such first-order task affinity can also be measured in the gradients during training [14, 18, 54]. These methods require training at most $k$ models but ignore higher-order structures, such as the transfer from a set of source tasks to the target. Thus, higher-order approximations that average the first-order task affinity are used as a substitute [42]. In our experiments, we have observed that the accuracy of averaging deteriorates as the size of $S$ grows (cf. Figure 1).

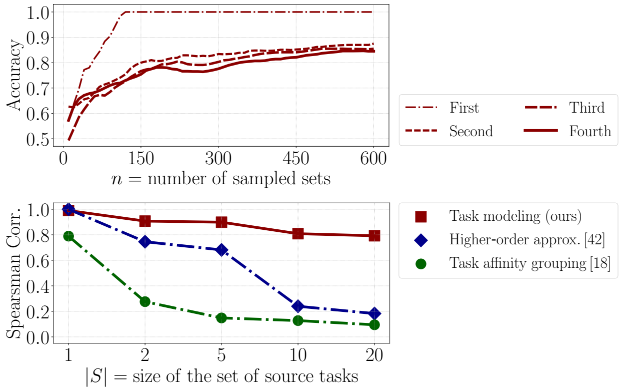

Figure 1: Will combining a set of source tasks $S$ with a primary target of interest help or hurt? We approach this question by sampling source tasks and estimating the loss of the target. This leads to a new way to efficiently approximate higher-order task structures, called *task modeling* in this work. **Top**: Task modeling answers the above question with 80% accuracy with up to four tasks in $S$. **Bottom:** Compared with existing higher-order approximations that average first-order task affinity [18, 42], task modeling consistently captures higher-order predictions more accurately.

In this work, we propose an efficient method to model first- and higher-order transfer predictions. Let $S$ be a subset of source tasks from $\{1, 2, \dots, k\}$. Our approach estimates a surrogate function to approximate the prediction loss of combining $S$ and a target task $t$, denoted as $f_t(S)$. If $S$ is similar to $t$, $f_t(S)$ will be small; otherwise $f_t(S)$ will be large. Thus, extrapolating such multitask predictions provides a way to model higher-order task structures. Our method, called *task modeling*, fits the value of $f_t(S)$ of $n$ random subsets $S$ with linear regression. Figure 1 shows that task modeling remains highly correlated with $f_t(S)$ as $|S|$ grows. Additionally, task modeling accurately predicts whether a set of source tasks transfer positively to the target.

**Results.** We prove that the sample complexity of task modeling is $O(k\alpha^4 \log^2 k)$ for any $|S|$ up to order $\alpha$ (cf. Theorem 2.1). In particular, task modeling requires comparable runtime to compute first-order task affinity, but accelerates computing higher-order affinity from $O(k^\alpha)$ to a nearly linear time in $k$. With task modeling as a surrogate function of $f_t(S)$, finding the optimal $S$ can be achieved with the task model, by selecting source tasks with negative model coefficients. The premise of this algorithm is that there exists one group of source tasks related to the target, while the rest are unrelated. In a linear parametric setting, we prove that our algorithm only selects related source tasks to the primary target task of interest (cf. Theorem 2.2).

We conduct a detailed empirical study of our methods on various datasets and performance metrics. First, we validate the benefit of modeling higher-order transfer for multitask learning and the efficiency of task modeling by detailing the computation costs. Second, we apply the task selection algorithm on five text classification tasks with noisy supervision sources [56], showing up to 3.6% accuracy improvement over all existing methods. Third, we show that task modeling can be used with group robustness and fairness metrics. On a tabular dataset where each task involves nine subpopulation groups [15], our approach consistently improves the worst-group accuracy over ten baselines.

**Summary.** This work presents a scalable sampling method to model higher-order task structures. Theoretical analysis shows that the sample complexity of the method is nearly linear in $k$ (cf. Theorem 2.1). By approximating multitask predictions, task modeling identifies source tasks whose prediction losses are small, thus are more related to the primary target task. The method shows promising results in text classification tasks with multiple noisy supervisions. It also applies to group robustness and fairness metrics. After discussing the related works, we will present our methodology in Section 2. Then, we describe our experiments in Section 3. We conclude our paper in Section 4.

### 1.1 Related work

Our work builds on and extends various settings studied in multitask learning (MTL) and transfer learning.

*Multitask Learning:* We build on existing MTL approaches using an architecture that shares the encoder for all tasks and assigns a separate predictor layer for each task [37]. These approaches have shown great progress in both language [29] and vision domains [32]. Meanwhile, many studies have observed negative results, where MTL performs worse than single task learning [45, 50]. This raises the question of identifying the negative interference and finding the task structures [55]. This is further complicated by the nonlinearity of neural networks. One approach is to measure gradient similarity during training [18, 54]. Since gradients are noisy, directly precomputing multitask predictions is considered [42], which computes first-order task affinity for all pairs of tasks and uses them to approximate higher-order transfer predictions. Our work offers an efficient and principled approach to model higher-order task structures via sampling. Some studies design neural net architectures to encourage information sharing across multiple tasks. Depending on the semantics, layers may be shared or separated across the network [22, 28, 59]. However, this approach requires specifying one architecture for each application. Low-rank tensor factorization can be used to constrain several task model parameters [49, 52]. Complementary to these works, we fix the network encoder and examine the relations of task data structures.

*Task Grouping:* Our setting is related to the task grouping problem [18, 26, 42], which is defined as assigning tasks into several groups with each learned in one network for optimizing the overall loss. Different from this problem, we are concerned with a primary target task of interest. This is also studied in several recent works [12, 14, 19, 38], and is loosely related to a robust multitask learning problem [11, 53] studied earlier within linear and kernel models.

*Generalization Theory:* Some of the earliest works in multitask learning study task relatedness from a learning theoretic perspective [7, 8]. Ben-David et al. [6] introduce a discrepancy notion called $H$-divergence, which leads to a generalization bound for minimizing the empirical risk of combining source and target training data. Transfer exponents are another measure of discrepancy between two distributions [21], leading to minimax convergence rates. Notice that our sample complexity bound only requires the Rademacher complexity of the encoder. Thus, they can also be combined with spectral norm bounds of deep networks [4], leading to a generalization bound for multitask learning with deep networks. Variants of the linear parametric model for task selection has also been considered in few-shot learning [16] and meta-learning [25]. Extending our approach to these cases is a promising research direction.

*Weak Supervision:* We draw motivation from recent work which models and integrates weak supervision for rapidly training deep models [2, 20, 24, 33, 39, 41]. In particular, our work is inspired by previous multitask weak supervision approaches [34, 36]. These approaches, however, do not handle the negative interference between multiple labeling functions. Our approach is related to probabilistic models of the noisy sources [27], but differ in that each label is treated as a source task rather than aggregated together.

## 2 Methodology

We present methods to model higher-order transfer and optimize cross-task transfer. Our approach estimates a surrogate function to approximate multitask prediction losses with linear regression. We show that such functions can be estimated efficiently and predict the losses accurately. Thus, optimizing cross-task transfer can be done using the task models, leading to an algorithm for selecting source tasks.

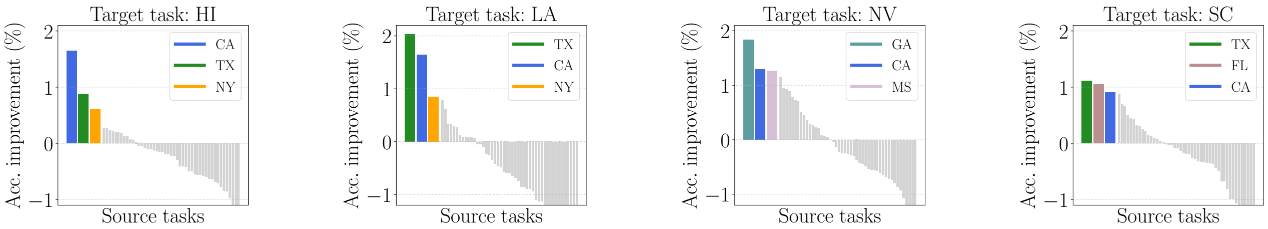

Figure 2: Mixed outcomes are commonly observed due to negative transfer in multitask learning. In some cases, combining a source task with a target task helps; in other cases, it hurts. $\boldsymbol{x}$**-axis**: Each bar represents one source task, for a total of fifty of them. $\boldsymbol{y}$**-axis**: Difference between test accuracy of combining a source and target task and single task learning.

### 2.1 Preliminaries

**Problem setup.** Consider a target task whose input features and class labels are drawn from an unknown distribution $\mathcal{D}_t$, supported on the product of a feature space $\mathcal{X}$ and a label space $\mathcal{Y}$. Suppose we have access to a training set $\hat{\mathcal{D}}_t$ and a validation set $\tilde{\mathcal{D}}_t$, both drawn from $\mathcal{D}_t$. Let $N$ be the size of the validation set $\tilde{\mathcal{D}}_t$. Given a predictor $f : \mathcal{X} \rightarrow \mathbb{R}^k$ and a nonnegative function $\ell : \mathbb{R}^k \times \mathcal{Y} \rightarrow \mathbb{R}^+$, the loss of a sample $x, y$ is denoted as $\ell(f(x), y)$.

Suppose we have access to $k$ related data distributions $\mathcal{D}_1, \mathcal{D}_2, \dots, \mathcal{D}_k$, called *source tasks*, which are supported on $\mathcal{X} \times \mathcal{Y}$. In cross-task transfer learning, we want to select a set of source tasks so that combining them with the target task optimizes the target task's performance. We assume that some of the source tasks are related to the target task, while many of them may negatively interfere (see Figure 2 for an example). Thus, the problem is to select the related tasks out of the $k$ source tasks.

A naive solution to this problem is to enumerate all combinations of source tasks. This requires training $2^k$ models, which is too costly. Another solution is to train $k$ models, one for every source-target pair. Select all source tasks that provide a positive transfer to the target task. This idea trades off precision for efficiency and underlies several existing multitask learning approaches [18, 42]. Given that several source tasks will be combined with the target task, higher-order structures need to be considered.

*Higher-order transfer:* To capture higher-order transfer, we will consider a distribution $\mathcal{S}$ supported on subsets of a fixed size $\alpha$. For instance, to capture how well five source tasks transfer to the target, $\mathcal{S}$ is a uniform distribution over subsets of $\{1, \dots, k\}$ with size five. Later in Section 2.3, we argue that this distribution enjoys a certain covariance structure that preserves the gap between related and unrelated tasks.

*Hard parameter sharing:* We will consider a popular architecture to combine the task samples but stress that our approach applies to other sharing architectures. Let $\phi$ be a shared encoder for all tasks. The encoder $\phi$ transforms a sample from the feature space $\mathcal{X}$ to a latent space. Each task including the target task uses a separate predictor, denoted as $\psi_1, \psi_2, \dots, \psi_{|S|}$, and $\psi_t$. Each predictor transforms the latent representation to a $k$ dimensional prediction. The optimization objective averages the loss of all samples.

**Notations.** Let $\mathrm{Id}_{p\times p}$ denote the identity matrix with dimension $p$ by $p$. Let $\|\cdot\|$ denote the Euclidean norm of a vector. For two functions $f(n)$ and $g(n)$, we write $g(n) \lesssim f(n)$ if there exists a fixed value $c$ that does not grow with $n$ such that $g(n) \leq c \cdot f(n)$ when $n$ is large enough. Let $\mathcal{F} = \{\ell(\psi_t(\phi(x)), y) \mid \forall\, \psi_t, \phi\}$ be a function class of the target task. Let $\mathcal{R}_N(\mathcal{F})$ be the Rademacher complexity of $\mathcal{F}$ on $N$ samples of the target task distribution.

### 2.2 Efficiently modeling higher-order transfer

We will estimate a surrogate function to approximate *multitask predictions*, which will be defined precisely below. Informally, this measures how well a set of source tasks transfer to the target task. We show that it is possible to approximate higher-order transfer predictions with sample complexity $O(k\alpha^4 \log^2 k)$. Our method has two steps:

i) **Evaluate multitask predictions:** For $i = 1, \dots, n$, sample $S_i$ from $\mathcal{S}$. Perform multitask training with the training samples in $S_i$. With a trained encode $\phi$ and the predictor $\psi_t$, evaluate the *multitask prediction* loss of $S_i$:

$$f_t(S_i) = \frac{1}{N} \sum_{(x,y)\in\tilde{\mathcal{D}}_t} \ell\big(\psi_t(\phi(x)), y\big). \qquad (1)$$

ii) **Estimate surrogate functions:** For $S \subseteq \{1, \dots, k\}$, let $g(S) = \theta^\top \mathbb{1}_S$, parametrized by a $k$ dimensional vector $\theta$, where $\mathbb{1}_S \in \{0,1\}^k$ be the characteristic vector of whether or not a task is in $S$.. With $n$ subsets and multitask predictions, estimate $\theta$ as:

$$\hat{\theta}_n \leftarrow \arg\min_{\theta\in\mathbb{R}^k} \hat{\mathcal{L}}_n(\theta) := \frac{1}{n} \sum_{i=1}^{n} \Big(\theta^\top \mathbb{1}_{S_i} - f_t(S_i)\Big)^2. \qquad (2)$$

*Theory.* We analyze the sample complexity of estimating $\hat{\theta}_n$. To formulate the problem, notice that the population risk can be defined by taking the expectation over the randomness of $f_t$:

$$\mathcal{L}(\theta) = \mathop{\mathbb{E}}_{f_t} \mathop{\mathbb{E}}_{T\sim\mathcal{S}} \Big[\Big(\theta^\top \mathbb{1}_T - f_t(T)\Big)^2\Big]. \qquad (3)$$

Let $\theta^\star$ be the population risk minimizer. Our result will depend on the Rademacher complexity of the function class. Additionally, we analyze the convergence of the empirical risk. Our result is stated below.

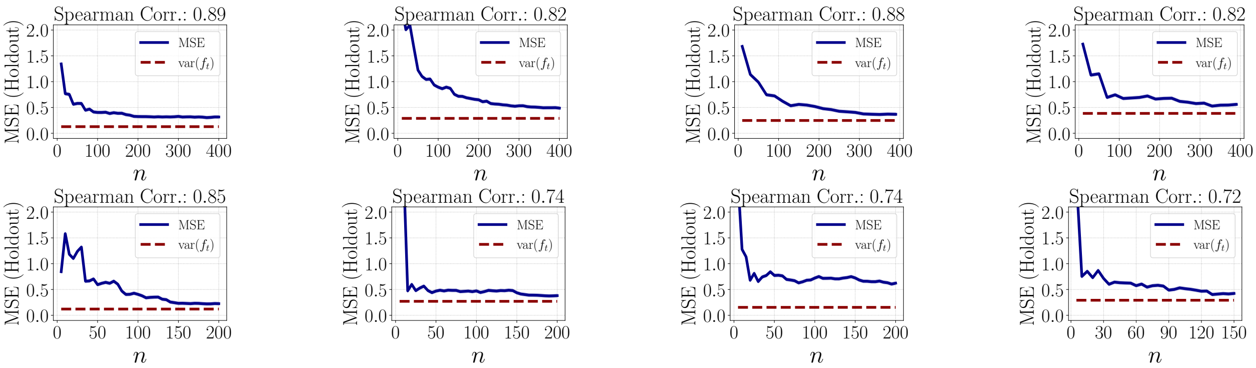

Figure 3: **(a)** The MSE of task modeling converges with less than $8k$ samples. **(b)** Task modeling approximates $f_t$ accurately with a Spearman correlation coefficient of 0.8 on average. **Top**: Training one binary classification target task along with subsets of **50** source tasks. **Bottom**: Training one text classification target task along with subsets of **24** source tasks.

**Theorem 2.1.** *Suppose the functions in $\mathcal{F}$ are bounded by a fixed $C$. Suppose $\alpha \le k/2$. With probability at least $1-\delta$, for any $\delta \ge 0$, $\hat{\theta}_n$ converges to $\theta^\star$:*

$$\left\|\hat{\theta}_n - \theta^\star\right\| \lesssim \mathcal{R}_N(\mathcal{F}) + \frac{\sqrt{\alpha \log(\delta^{-1}k)}}{\sqrt{N}} + \frac{C\alpha^2 \log(\delta^{-1}k)\sqrt{k}}{\sqrt{n}} + \frac{C\alpha\sqrt{\delta^{-1}k}}{\sqrt{n}}. \tag{4}$$

*$\hat{\theta}_n$'s empirical risk converges to $\theta^\star$'s population risk:*

$$\mathcal{L}(\theta^\star) - \hat{\mathcal{L}}_n(\hat{\theta}_n) \lesssim C\alpha \cdot \mathcal{R}_N(\mathcal{F}) + \frac{C\alpha^{3/2}\sqrt{\log(\delta^{-1}k)}}{\sqrt{N}} + \frac{C^2\alpha^{7/2}\log(\delta^{-1}k)\sqrt{k}}{\sqrt{n}} + \frac{C^2\alpha^{5/2}\sqrt{\delta^{-1}k}}{\sqrt{n}}. \tag{5}$$

This theorem implies that the sample complexity of estimating linear task models is only $O(k\alpha^4 \log^2 k)$—a nearly linear rate in the number of tasks. While the constants in equations (4) and (5) can be large, our empirical result suggests that they are small in practice. More broadly, the complexity bound works under mild conditions of the loss. Later in Section 3.3, we show similar results for several group robustness and fairness measures in place of $f_t$. The proof of Theorem 2.1 is presented in Appendix A.1.

**Empirical examples.** We validate that the above procedure estimates an accurate approximation of $f_t$ efficiently. We consider tabular and text datasets, respectively. For the tabular dataset, there are 50 source tasks. For the text dataset, there are 24 source tasks. We evaluate the task model $g$ on a holdout set. In both cases, we consider five-way multitask relations, i.e., $\mathcal{S}$ is a uniform distribution over all combinations of source tasks with size $\alpha = 5$. For tabular datasets, we use a fully-connected layer as the encoder. For text datasets, we use BERT-mini as the encoder. The rest of the setup is deferred to Section 3.1.

Figure 3 plots the convergence of task modeling for eight target tasks—more results can be found in Appendix B.1, which are similar. We find that in all cases, with $n \le 8k$, the MSE of $\hat{\theta}_n$ on a holdout set converges comparably to the variance of $f_t$. The variance of $f_t$ over a random subset $T$ of $\mathcal{S}$ is defined as

$$\operatorname{var}(f_t) = \frac{1}{n}\sum_{i=1}^{n}\left(f_t(S_i) - \mathop{\mathbb{E}}_{f_t}\left[f_t(S_i)\right]\right)^2. \tag{6}$$

We estimate the empirical mean of $f_t$ with the average value over 10 random seeds. Note that a smaller gap between the empirical risk and the variance of $f_t$ implies the linear model fits the expected $f_t$ values more accurately. The Spearman correlation between $f_t(\cdot)$ and $g(\cdot)$ is 0.8 averaged over the eight cases. See Appendix B.2 for similar results with more target tasks.

*Remark.* The above procedure is inspired by a recent work of Ilyas et al. [23], which predicts the prediction of a set of training samples on another sample drawn from the same unknown distribution. Notice that the multitask learning setting crucially differs from the above work, since we estimate the prediction of combining a subset of source tasks with a target task, then test on the target task.

### 2.3 Optimizing cross-task transfer learning

Optimize cross-task transfer performance requires finding an $S$ that minimizes $f_t(S)$. With a task model, we can select $S$ using the approximated model: $S^\star = \arg\min_S g(S)$. Thus, the minimum can be achieved by choosing all source tasks with a negative coefficient in $\hat{\theta}_n$. Due to the stochasticity of $\hat{\theta}_n$, in practice, we set a threshold $\gamma$ instead. The complete procedure is summarized in Algorithm 1.

*Theory.* To illustrate the intuition behind the above algorithm, we present a case study in a toy parametric model. Assume the feature covariate of every task is drawn from an isotropic normal distribution $\mathcal{N}(0, \mathrm{Id}_{p\times p})$. Each task $i$ follows a linear model specified by a parameter vector $\theta^{(i)}$. Given a $p$ dimensional feature vector $x$, the label of task $i$ satisfies $y = x^\top\theta^{(i)} + \epsilon$, where $\epsilon$ is a random variable with mean 0 and variance $\sigma^2$. Let $a$ and $b$ be two fixed values so that $b > a > 0$, a task is:

- *related* if $\theta^{(i)} = \theta^{(t)} + z$, where $z \sim \mathcal{N}(0, a^2\,\mathrm{Id}_{p\times p})$;
- *unrelated* if $\theta^{(i)} = \theta^{(t)} + z$, where $z \sim \mathcal{N}(0, b^2\,\mathrm{Id}_{p\times p})$.

```
Algorithm 1: Selecting source tasks using task modeling
Input: A set of training data samples from each source task $\hat{\mathcal{D}}_1, \ldots, \hat{\mathcal{D}}_k$; A training and validation set of the target task $\hat{\mathcal{D}}_t$ and $\tilde{\mathcal{D}}_t$.
Require: A multitask prediction loss function $f_t : 2^{\{1,2,\ldots,k\}} \rightarrow \mathbb{R}^+$; A distribution over subsets of source tasks $\mathcal{S}$; Number of subsets $n$; A threshold $\gamma$.
Output: A subset of tasks $S^\star \subseteq \{1, 2, \ldots, k\}$.
1: For $i = 1, \ldots, n$, sample a set $S_i$ from $\mathcal{S}$, perform multitask
   training to get $\psi_t, \phi$, and evaluate $f_t(S_i)$.
2: Estimate the task model coefficients $\hat{\theta}_n$ following equation 2.
3: Select source tasks: $S^\star = \{i : \hat{\theta}_n(i) < \gamma, \text{ for any } 1 \le i \le k\}$.
```

We prove that with enough samples, Algorithm 1 only selects related source tasks.

**Theorem 2.2.** *In the setting described within this subsection, suppose the loss function $\ell$ is bounded from above by $C > 0$. There are $d$ samples from each task. Let $n \gtrsim C^2k^2/((a^2 - b^2)^2))$, $d \gtrsim a^4k^4/(a^2 - b^2)^2 + k \log k + p$, and $N \gtrsim p \log p$. There exists a threshold $\gamma$ such that with probability at least* 0.99*,*

- *$\hat{\theta}_n(i) < \gamma$ for any related task $i \in \{1, 2, \ldots, k\}$;*
- *$\hat{\theta}_n(j) > \gamma$ for any unrelated task $j \in \{1, 2 \ldots, k\}$.*

The analysis of Theorem 2.2 uses the fact that $\mathcal{S}$ is a uniform distribution over subsets of a fixed size. We show that under this distribution, the covariance structure in the task indices of $\hat{\theta}_n$ is approximately an identity matrix plus a constant term for every task (cf. Lemma A.3). This covariance structure allows the task model coefficients to separate the related tasks from the unrelated tasks (i.e., amplifying the gap between $a$ and $b$). More details of the setting and the proof of Theorem 2.2 are deferred to Appendix A.2.

# 3 Experiments

Our experiments seek to address the following questions: (i) Does modeling higher-order transfers in task modeling bring some benefit compared to prior works using first-order task affinity? (ii) Does our approach select tasks that transfer positively to the target task? (iii) How well does our approach extend to performance metrics beyond the average prediction loss?

We investigate these questions on various datasets and performance metrics, showing positive results to the three questions. First, we present a detailed analysis of task modeling to validate the benefit of higher-order transfers over first-order transfer metrics and report the computational cost of our approach. Second, we apply our approach to five text classification tasks with noisy supervision sources. Our approach increases the test performance over combining all tasks by **6.4%** and prior methods up to **3.6%**. Third, we apply our approach to optimize group robustness and fairness measures on datasets with multiple subgroups. Our approach consistently improves performance over previous multitask learning approaches on six target tasks.

## 3.1 Experimental setup

**Datasets.** First, we consider text classification tasks with noisy supervision sources from a weak supervision dataset [56]. Each weak supervision source generates noisy labels for a subset of training samples. We view noisy sources as source tasks. The task with true labels can be viewed as the target task and is not available during training. A validation set of true labels is used for task selection and parameter tuning. Table 1 describes the statistics of five text classification tasks along with the number of source tasks.

Table 1: Dataset statistics of five text classification tasks.

| Tasks | Youtube | TREC | CDR | Chemprot | Semeval |
|---|---|---|---|---|---|
| Training | 1,586 | 4,965 | 8,430 | 12,861 | 1,749 |
| Validation | 120 | 500 | 920 | 1,607 | 178 |
| Test | 250 | 500 | 4,673 | 1,607 | 600 |
| Source tasks | 10 | 68 | 33 | 26 | 164 |

Second, we consider binary classification tasks which involve multiple groups of subpopulations. We consider the Folktables dataset derived from the US census [15], in particular an income prediction task spanning all states. In this task, each record indicates whether an individual's income is above $50,000 or not, using ten tabular features including education level, age, sex, etc. We view each state as one task. We use the racial attribute of an individual to split each state dataset into nine groups that exhibit group shifts. We evaluate the robustness of a predictor with its worst-group accuracy, defined as the predictor's accuracy in the worst performing group among all nine groups. Table 2 describes the statistics of six states/target tasks. In each case, there will be fifty source tasks.

Table 2: Dataset statistics of six binary classification tasks.

| Tasks | HI | KS | LA | NJ | NV | SC |
|---|---|---|---|---|---|---|
| Training | 4,638 | 9,484 | 12,400 | 28,668 | 8,884 | 14,927 |
| Validation | 1,546 | 3,161 | 4,133 | 9,556 | 2,961 | 4,976 |
| Test | 1,547 | 3,162 | 4,134 | 9,557 | 2,962 | 4,976 |
| Smallest group | 67 | 75 | 58 | 52 | 61 | 203 |

**Baselines.** We first compare our approach with training on all tasks using hard parameter sharing. Then, we consider approaches that model first-order task affinity, including approximating higher order task relations using two-task network performance [42], estimating task relations using cosine similarity between task gradients [18] and computing lookahead losses with task gradients [18]. Additionally, we also consider approaches that alter the optimization using pairwise task relations, including auxiliary task gradient update decomposition [14] and target-aware weighted training [12].

For tasks with weak supervision sources, we incorporate previous weak supervision methods to aggregate noisy labels and train an end model on the labels inferred by the methods. The methods include Majority Vote, Data Programming [35], and MeTaL [34].

Table 3: Test performance on five text classification tasks with multiple noisy supervisions, averaged over five random seeds.

| Method/Dataset (Metrics) | Youtube (Acc.) | TREC (Acc.) | CDR (F1) | Chemprot (Acc.) | Semeval (Acc.) | Avg. Rank |
|---|---|---|---|---|---|---|
| Majority Vote | 95.36±1.71 | 66.56±2.31 | 58.89±0.50 | 57.32±0.98 | 85.03±0.83 | 4.6 |
| Data Programming [35] | 93.84±1.61 | 68.64±3.57 | 58.48±0.73 | 57.00±1.20 | 83.93±0.83 | 6.6 |
| MeTaL [34] | 92.32±1.44 | 58.28±1.95 | 58.48±0.90 | 56.17±0.66 | 71.74±0.57 | 8.4 |
| Hard parameter sharing | 94.72±0.85 | 64.10±0.50 | 58.20±0.55 | 53.43±0.53 | 89.00±1.06 | 7.8 |
| High-order approx. [42] | 94.93±1.80 | 74.67±4.66 | 59.76±0.97 | 45.57±0.41 | 79.94±4.42 | 6.2 |
| Gradient similarity [18] | 95.33±0.68 | 78.25±3.71 | 59.21±0.80 | 53.67±1.89 | 89.89±2.17 | 4.0 |
| Task affinity grouping [18] | 95.20±0.65 | 77.50±3.62 | 59.31±0.15 | 53.67±2.74 | 89.06±1.47 | 4.2 |
| Weighted training [12] | 94.53±1.05 | 72.40±2.36 | 59.85±0.30 | 53.76±2.96 | 86.83±1.78 | 5.0 |
| Gradient decomposition [14] | 95.28±0.16 | 65.80±1.81 | 58.81±0.36 | 54.76±0.67 | 78.57±0.13 | 7.0 |
| **Task modeling (Alg. 1)** | **97.47±0.82** | **81.80±1.14** | **61.22±0.39** | **57.54±0.55** | **93.50±0.24** | **1.0** |

For the binary prediction tasks, we also consider empirical risk minimization and approaches that aim to improve the worst-group performance, including importance weighting [9], group distributionally robust optimization [40], and supervised contrastive learning [57]. More details concerning hyperparameters are described in Section B.1.

**Implementation.** We use BERT-Base on the text classification tasks. For the income prediction task from the Folktables dataset, we use a two-layer perceptron model with a hidden size 32. We adopt the hard parameter sharing architecture for conducting multitask learning on the datasets.

To estimate a task model, we collect $n$ task subsets along with the multitask training result of each subset. We consider a uniform sampling distribution over the task subsets of a constant size. For each income prediction task, we obtain $n = 400$ results on $|S| = 5$ source tasks. We also construct as a holdout set of size 100. For the text classification datasets, since the number of source tasks (c.f. Table 1) varies among datasets. We obtain $n = \{50, 200, 200, 400, 800\}$ results with each on $|S| = \{3, 5, 5, 10, 15\}$ source tasks from Youtube, Chemprot, CDR, TREC, Semeval datasets, respectively. We set $f_t(S)$ as the negative classification margin — the difference between the logit of the correct class and the highest incorrect logit.

## 3.2 Task modeling results

*How much does modeling higher-order structures gain?* We validate the benefit of using higher-order task affinity over first-order and second-order task affinities.

For first-order task affinity, we select source tasks by training every source task with the target task, following HOA [42]. The results in Table 3 and 4 confirm that by sampling subsets of $S$ with size up to five, task modeling outperforms HOA by **3.9%** averaged over eleven tasks.

For second-order task affinity, we conduct an exhaustive search over the space of source tasks to show that going beyond first-order task affinity is necessary. We search through all possible choices of $|S| = 2$ on one binary classification task, which amounts to training 1225 models, each with two source tasks and one target task. The results show that our approach outperforms the best $S$ by **1.21%** accuracy. See Table 6 of Appendix B.3 for the results.

*How long does constructing task models take?* We detail the computation costs of our approach. As shown in Section 2.2, for each target task, using $n \le 8k$ subsets suffices for task models to converge. We validate similar convergence for other tasks in Figure 5 of Appendix B.2. We also report the GPU hours of collecting training results for each target task in Appendix B.3. Across all eleven cases, constructing task models until convergence takes at most 85.9 GPU hours, evaluated on an NVIDIA TITAN RTX instance.

Next, we compare the computation costs of task modeling and prior methods. We use one binary classification task as an example. To only precompute first-order task affinity, our approach takes the same amount of time as HOA, which takes 1.24 GPU hours to train on all source-target pairs, and comparable time to TAG, which takes 0.87 GPU hours.

Notice that both HOA and TAG are not designed to predict higher-order transfers. Thus, we compare our approach with exhaustive search for $|S| > 2$. Recall that our approach requires sampling $n = O(k\alpha^4 \log^2 k)$ in theory. In practice, we notice that $n = 8k$ suffices for training task models until convergence in all of our use cases. We also notice that the required $n$ decreases as $|S|$ increases, as shown in Figure 4 of Section 3.2. As a result, our approach takes the same amount of time for different sizes of $S$ up to 20, which is less than 52 GPU hours. By contrast, the runtime of the exhaustive search increases exponentially as the size of $S$ grows.

## 3.3 Task selection results

**Cross-task transfer learning.** Our result in Section 2.3 shows that task modeling provides signals to identify beneficial source tasks. We validate the result with the text classification tasks with several noisy supervision sources. We apply Algorithm 1 to select the noisy sources and evaluate the test performance on the classification task with true labels. Table 3 shows the results.

Compared with hard parameter sharing which trains all tasks in the same network, our algorithm improves the test performance by **6.4%** on average. This shows that our algorithm excludes tasks with negative interference, thus performing better than training on all tasks. Compared with existing multitask learning approaches that either reweight the source tasks [12, 14] or select with first-order task affinity [18, 42], our algorithm increases up to **3.6%** accuracy.

Table 4: Worst-group test accuracy on six binary classification tasks with tabular features, averaged over ten random seeds.

| Method/Dataset | HI | KS | LA | NJ | NV | SC | Avg. Rank |
|---|---|---|---|---|---|---|---|
| Empirical risk minimization | 74.46±0.48 | 73.73±1.19 | 72.39±1.96 | 76.34±0.64 | 72.89±1.42 | 75.20±1.07 | 9.7 |
| Importance weighting [9] | 74.53±0.81 | 72.84±1.74 | 74.82±0.94 | 76.43±0.50 | 71.25±1.73 | 75.30±0.05 | 7.8 |
| Correct-N-Contrast [57] | 74.37±0.27 | 75.52±1.19 | 74.25±0.15 | 77.60±0.10 | 73.22±0.40 | 76.23±0.98 | 5.0 |
| Group robust optimization [40] | 74.56±0.58 | 75.50±0.59 | 74.90±0.38 | 76.95±0.20 | 73.06±0.66 | 75.56±1.36 | 5.5 |
| Hard parameter sharing | 73.63±0.46 | 75.22±0.73 | 73.24±1.01 | 77.28±0.25 | 73.22±1.12 | 76.23±0.49 | 8.0 |
| High-order approx. [42] | 74.67±0.32 | 75.22±1.48 | 73.69±0.86 | 77.49±0.25 | 73.88±0.66 | 76.80±0.65 | 3.6 |
| Gradient similarity [18] | 74.53±0.52 | 75.22±2.02 | 73.66±1.22 | 77.44±0.38 | 74.38±0.91 | 77.03±0.54 | 3.8 |
| Task affinity grouping [18] | 74.48±0.41 | 75.97±1.18 | 73.24±1.01 | 77.41±0.48 | 74.05±0.84 | 76.41±0.50 | 5.1 |
| Weighted training [12] | 73.53±0.44 | 75.14±1.39 | 73.51±1.38 | 76.47±1.31 | 72.89±0.81 | 76.59±0.97 | 7.8 |
| Gradient decomposition [14] | 73.20±0.57 | 72.24±1.19 | 73.51±0.66 | 76.38±0.69 | 73.71±0.84 | 76.77±0.66 | 8.0 |
| **Task modeling (Alg. 1)** | **75.47±0.73** | **76.96±0.69** | **75.62±0.11** | **78.17±0.36** | **75.21±0.52** | **77.62±0.34** | **1.0** |

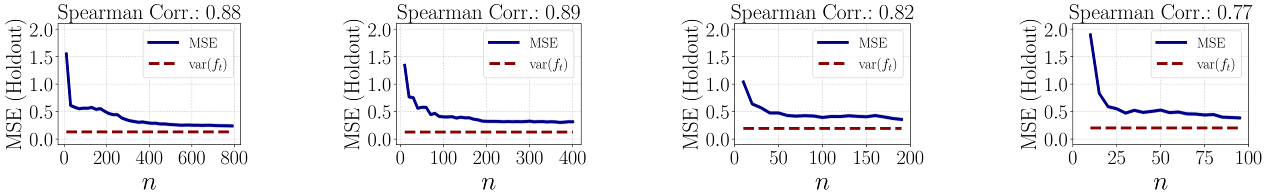

Figure 4: Ablation study of choosing different subset sizes on the same target task. From left to right: $|S| = 2, 5, 10, 20$.

**Group robustness and fairness metrics.** Next, we show that task modeling also captures task affinity with various performance metrics of the primary target task. We consider the binary classification tasks with multiple subpopulation groups. We apply Algorithm 1 to select source tasks as an augmentation of the target classification task. Table 4 presents the comparison of the worst-group accuracy.

Compared with single task learning, including ERM, GroupDRO, and CNC, we find that task modeling improves the worst-group accuracy by 1.17% on average, confirming the benefit of data augmentation. Compared with existing multitask learning approaches, our approach shows a favorable gain of up to **1.9%** absolute accuracy. On two fairness measures, our algorithm outperforms all methods by **1.8%** on average. Due to the space limit, this result is described in Appendix B.3. Hence, we conclude that task modeling is a general approach that approximates multitask predictions for various performance measures.

### 3.4 Ablation study of model parameters

We ablate the parameters used in our algorithm, providing further insights into its working.

*Subset size $|S|$:* Recall that we collect training results by sampling $n$ subsets from a uniform distribution over subsets of a constant size. We evaluate the MSE of task models by varying $|S| \in \{2, 5, 10, 20\}$. To control the computation budget the same, we scale the number of subsets $n$ according to $|S|$. We train $n = 800, 400, 200, 100$ models with $|S| = 2, 5, 10, 20$, respectively. We observe similar convergence results as in Figure 3. Among them, $|S| = 5$ yields a highest Spearman correlation of 0.89 between $f_t(\cdot)$ and $g(\cdot)$. The reason why higher values of $|S|$ do not help is that the number of beneficial tasks is limited in this setting.

*Number of samples $n$:* Next, we explore how $n$ affects the estimated task models. We measure the effect on two tasks (HI and LA) by comparing the 10 tasks with the smallest coefficients estimated from $n = 100, 200, 400$ subsets. We observe that using 100 subsets identifies 7 (out of 10) same source tasks as using 400. Increasing $n$ to 200 further identifies 9 (out of 10) same source tasks as using 400.

*Loss function $\ell$:* We consider three choices of prediction losses, including zero-one accuracy, cross-entropy loss, and classification margin. We observe that using the classification margin is more effective than the other two metrics. The Spearman correlation of using the margin is 0.86 on average over two tasks (HI and LA). In contrast, the Spearman correlations of using the loss and accuracy are 0.61 and 0.34, respectively. Besides, we compare the task selection using the three metrics in Table 6. We find that using the margin outperforms the other two by 0.37% on average over the six target tasks in terms of worst-group accuracy.

## 4 Conclusion

We propose task modeling to capture first- and higher-order task transfers. This approach extrapolates multitask predictions by sampling task subsets and estimating a surrogate function of the prediction losses. Our empirical and theoretical results demonstrate that task modeling accurately predicts multitask prediction losses with only linear number of samples. This finding leads us to design an algorithm for cross-task transfer learning using task modeling. We validate our approach on text and tabular classification tasks with various performance metrics. Experiments show that our approach effectively improves both the average and group robust metrics. Our work highlights the benefit of modeling higher-order transfers in multitask learning.

# References

[1] Andreas Argyriou, Theodoros Evgeniou, and Massimiliano Pontil. “Convex multi-task feature learning”. In: *Machine learning* 73.3 (2008), pp. 243–272.

[2] Stephen H Bach, Daniel Rodriguez, Yintao Liu, Chong Luo, Haidong Shao, Cassandra Xia, Souvik Sen, Alex Ratner, Braden Hancock, Houman Alborzi, et al. “Snorkel drybell: A case study in deploying weak supervision at industrial scale”. In: *ICMD*. 2019, pp. 362–375.

[3] Francesco Barbieri, Jose Camacho-Collados, Luis Espinosa Anke, and Leonardo Neves. “TweetEval: Unified Benchmark and Comparative Evaluation for Tweet Classification”. In: *EMNLP*. 2020, pp. 1644–1650.

[4] Peter L Bartlett, Dylan J Foster, and Matus J Telgarsky. “Spectrally-normalized margin bounds for neural networks”. In: *NeurIPS* 30 (2017).

[5] Peter L Bartlett and Shahar Mendelson. “Rademacher and Gaussian complexities: Risk bounds and structural results”. In: *Journal of Machine Learning Research* 3.Nov (2002), pp. 463–482.

[6] Shai Ben-David, John Blitzer, Koby Crammer, Alex Kulesza, Fernando Pereira, and Jennifer Wortman Vaughan. “A theory of learning from different domains”. In: *Machine learning* 79.1 (2010), pp. 151–175.

[7] Shai Ben-David and Reba Schuller Borbely. “A notion of task relatedness yielding provable multiple-task learning guarantees”. In: *Machine learning* 73.3 (2008), pp. 273–287.

[8] Shai Ben-David and Reba Schuller. “Exploiting task relatedness for multiple task learning”. In: *Learning theory and kernel machines*. Springer, 2003, pp. 567–580.

[9] Jonathon Byrd and Zachary Lipton. “What is the effect of importance weighting in deep learning?” In: *ICML*. 2019, pp. 872–881.

[10] Rich Caruana. “Multitask learning”. In: *Machine learning* (1997).

[11] Jianhui Chen, Jiayu Zhou, and Jieping Ye. “Integrating low-rank and group-sparse structures for robust multi-task learning”. In: *KDD*. 2011, pp. 42–50.

[12] Shuxiao Chen, Koby Crammer, Hangfeng He, Dan Roth, and Weijie J Su. “Weighted Training for Cross-Task Learning”. In: *ICLR* (2022).

[13] Koby Crammer, Michael Kearns, and Jennifer Wortman. “Learning from Multiple Sources.” In: *Journal of Machine Learning Research* 9.8 (2008).

[14] Lucio M Dery, Yann Dauphin, and David Grangier. “Auxiliary task update decomposition: The good, the bad and the neutral”. In: *ICLR* (2021).

[15] Frances Ding, Moritz Hardt, John Miller, and Ludwig Schmidt. “Retiring adult: New datasets for fair machine learning”. In: *NeurIPS* 34 (2021).

[16] Simon S Du, Wei Hu, Sham M Kakade, Jason D Lee, and Qi Lei. “Few-shot learning via learning the representation, provably”. In: *ICML* (2020).

[17] Theodoros Evgeniou and Massimiliano Pontil. “Regularized multi–task learning”. In: *Proceedings of the tenth ACM SIGKDD international conference on Knowledge discovery and data mining*. 2004, pp. 109–117.

[18] Chris Fifty, Ehsan Amid, Zhe Zhao, Tianhe Yu, Rohan Anil, and Chelsea Finn. “Efficiently identifying task groupings for multi-task learning”. In: *NeurIPS* 34 (2021).

[19] Han Guo, Ramakanth Pasunuru, and Mohit Bansal. “AutoSeM: Automatic Task Selection and Mixing in Multi-Task Learning”. In: *NAACL* (2019).

[20] Bo Han, Quanming Yao, Xingrui Yu, Gang Niu, Miao Xu, Weihua Hu, Ivor Tsang, and Masashi Sugiyama. “Co-teaching: Robust training of deep neural networks with extremely noisy labels”. In: *NeurIPS* 31 (2018).

[21] Steve Hanneke and Samory Kpotufe. “On the value of target data in transfer learning”. In: *NeurIPS* 32 (2019).

[22] Jui-Ting Huang, Jinyu Li, Dong Yu, Li Deng, and Yifan Gong. “Cross-language knowledge transfer using multilingual deep neural network with shared hidden layers”. In: *ICASSP*. IEEE. 2013, pp. 7304–7308.

[23] Andrew Ilyas, Sung Min Park, Logan Engstrom, Guillaume Leclerc, and Aleksander Madry. “Datamodels: Predicting predictions from training data”. In: *ICML* (2022).

[24] Ashish Khetan, Zachary C Lipton, and Anima Anandkumar. “Learning from noisy singly-labeled data”. In: *ICLR* (2018).

[25] Weihao Kong, Raghav Somani, Zhao Song, Sham Kakade, and Sewoong Oh. “Meta-learning for mixed linear regression”. In: *International Conference on Machine Learning*. PMLR. 2020, pp. 5394–5404.

[26] Abhishek Kumar and Hal Daume III. “Learning task grouping and overlap in multi-task learning”. In: *ICML* (2012).

[27] Hunter Lang and Hoifung Poon. “Self-supervised self-supervision by combining deep learning and probabilistic logic”. In: *AAAI*. Vol. 35. 6. 2021, pp. 4978–4986.

[28] Xiaodong Liu, Jianfeng Gao, Xiaodong He, Li Deng, Kevin Duh, and Ye-Yi Wang. “Representation learning using multi-task deep neural networks for semantic classification and information retrieval”. In: *NAACL* (2015).

[29] Xiaodong Liu, Pengcheng He, Weizhu Chen, and Jianfeng Gao. “Multi-Task Deep Neural Networks for Natural Language Understanding”. In: *ACL*. 2019, pp. 4487–4496.

[30] Yixin Nie, Adina Williams, Emily Dinan, Mohit Bansal, Jason Weston, and Douwe Kiela. “Adversarial NLI: A New Benchmark for Natural Language Understanding”. In: *ACL*. 2020, pp. 4885–4901.

[31] Sinno Jialin Pan and Qiang Yang. “A survey on transfer learning”. In: *IEEE Transactions on knowledge and data engineering* (2009).

[32] Pranav Rajpurkar, Jeremy Irvin, Kaylie Zhu, Brandon Yang, Hershel Mehta, Tony Duan, Daisy Ding, Aarti Bagul, Curtis Langlotz, Katie Shpanskaya, et al. “Chexnet: Radiologist-level pneumonia detection on chest x-rays with deep learning”. In: *arXiv preprint arXiv:1711.05225* (2017).

[33] Alexander Ratner, Stephen H Bach, Henry Ehrenberg, Jason Fries, Sen Wu, and Christopher Ré. “Snorkel: Rapid training data creation with weak supervision”. In: *VLDB*. Vol. 11. 3. NIH Public Access. 2017, p. 269.

[34] Alexander Ratner, Braden Hancock, Jared Dunnmon, Frederic Sala, Shreyash Pandey, and Christopher Ré. “Training complex models with multi-task weak supervision”. In: *AAAI*. Vol. 33. 01. 2019, pp. 4763–4771.

[35] Alexander J Ratner, Christopher M De Sa, Sen Wu, Daniel Selsam, and Christopher Ré. “Data programming: Creating large training sets, quickly”. In: *NeurIPS* 29 (2016).

[36] Alexander J Ratner, Braden Hancock, and Christopher Ré. “The Role of Massively Multi-Task and Weak Supervision in Software 2.0.” In: *CIDR*. 2019.

[37] Sebastian Ruder. “An overview of multi-task learning in deep neural networks”. In: *arXiv preprint arXiv:1706.05098* (2017).

[38] Khaled Saab, Sarah M Hooper, Nimit S Sohoni, Jupinder Parmar, Brian Pogatchnik, Sen Wu, Jared A Dunnmon, Hongyang R Zhang, Daniel Rubin, and Christopher Ré. “Observational supervision for medical image classification using gaze data”. In: *MICCAI*. Springer. 2021, pp. 603–614.

[39] Esteban Safranchik, Shiying Luo, and Stephen Bach. “Weakly supervised sequence tagging from noisy rules”. In: *Proceedings of the AAAI Conference on Artificial Intelligence*. Vol. 34. 04. 2020, pp. 5570–5578.

[40] Shiori Sagawa, Pang Wei Koh, Tatsunori B Hashimoto, and Percy Liang. “Distributionally robust neural networks for group shifts: On the importance of regularization for worst-case generalization”. In: *ICLR* (2020).

[41] Changho Shin, Winfred Li, Harit Vishwakarma, Nicholas Roberts, and Frederic Sala. “Universalizing weak supervision”. In: *ICLR* (2022).

[42] Trevor Standley, Amir Zamir, Dawn Chen, Leonidas Guibas, Jitendra Malik, and Silvio Savarese. “Which tasks should be learned together in multi-task learning?” In: *ICML*. PMLR. 2020, pp. 9120–9132.

[43] Joel A Tropp. “An Introduction to Matrix Concentration Inequalities”. In: *Foundations and Trends in Machine Learning* 8.1-2 (2015), pp. 1–230.

[44] Roman Vershynin. “Spectral norm of products of random and deterministic matrices”. In: *Probability theory and related fields* 150.3 (2011), pp. 471–509.

[45] Tu Vu, Tong Wang, Tsendsuren Munkhdalai, Alessandro Sordoni, Adam Trischler, Andrew Mattarella-Micke, Subhransu Maji, and Mohit Iyyer. “Exploring and predicting transferability across NLP tasks”. In: *EMNLP* (2020).

[46] Martin J Wainwright. *High-dimensional statistics: A non-asymptotic viewpoint*. Vol. 48. Cambridge University Press, 2019.

[47] Alex Wang, Yada Pruksachatkun, Nikita Nangia, Amanpreet Singh, Julian Michael, Felix Hill, Omer Levy, and Samuel Bowman. “Superglue: A stickier benchmark for general-purpose language understanding systems”. In: *NeurIPS* 32 (2019).

[48] Alex Wang, Amanpreet Singh, Julian Michael, Felix Hill, Omer Levy, and Samuel Bowman. “GLUE: A Multi-Task Benchmark and Analysis Platform for Natural Language Understanding”. In: *ICLR*. 2019, pp. 353–355.

[49] Kishan Wimalawarne, Masashi Sugiyama, and Ryota Tomioka. “Multitask learning meets tensor factorization: task imputation via convex optimization”. In: *NeurIPS* 27 (2014).

[50] Sen Wu, Hongyang R Zhang, and Christopher Ré. “Understanding and improving information transfer in multi-task learning”. In: *ICLR* (2020).

[51] Fan Yang, Hongyang R Zhang, Sen Wu, Weijie J Su, and Christopher Ré. “Analysis of information transfer from heterogeneous sources via precise high-dimensional asymptotics”. In: *arXiv preprint arXiv:2010.11750* (2021).

[52] Yongxin Yang and Timothy Hospedales. “Deep multi-task representation learning: A tensor factorisation approach”. In: *ICLR* (2017).

[53] Shipeng Yu, Volker Tresp, and Kai Yu. “Robust multi-task learning with t-processes”. In: *ICML*. 2007, pp. 1103–1110.

[54] Tianhe Yu, Saurabh Kumar, Abhishek Gupta, Sergey Levine, Karol Hausman, and Chelsea Finn. “Gradient surgery for multi-task learning”. In: *NeurIPS* 33 (2020), pp. 5824–5836.

[55] Amir R Zamir, Alexander Sax, William Shen, Leonidas J Guibas, Jitendra Malik, and Silvio Savarese. “Taskonomy: Disentangling task transfer learning”. In: *CVPR*. 2018, pp. 3712–3722.

[56] Jieyu Zhang, Yue Yu, Yinghao Li, Yujing Wang, Yaming Yang, Mao Yang, and Alexander Ratner. “WRENCH: A Comprehensive Benchmark for Weak Supervision”. In: *NeurIPS Datasets and Benchmarks Track*. 2021.

[57] Michael Zhang, Nimit S Sohoni, Hongyang R Zhang, Chelsea Finn, and Christopher Ré. “Correct-N-Contrast: A Contrastive Approach for Improving Robustness to Spurious Correlations”. In: *ICML* (2022).

[58] Yu Zhang and Dit-Yan Yeung. “A convex formulation for learning task relationships in multi-task learning”. In: *UAI* (2010).

[59] Zhanpeng Zhang, Ping Luo, Chen Change Loy, and Xiaoou Tang. “Facial landmark detection by deep multi-task learning”. In: *ECCV*. Springer. 2014, pp. 94–108.

# A Proofs of Theorems 2.1 and 2.2

**Notations:** We follow the convention of big-O notations in the proof. Given two functions $f(n)$ and $g(n)$, we use $f(n) = O(g(n))$ to indicate that $f(n) \le C \cdot g(n)$ for some fixed constant $C$ when $n$ is large enough. The notation $f(n) \lesssim g(n)$ indicates that $f(n) = O(g(n))$. We use $f(n) = (1 + o(1))g(n)$ to indicate that $|f(n) - g(n)|/g(n)$ approaches zero as $n$ goes to infinity.

For a matrix $X$, denote the spectral norm (or the largest singular value) of $X$ as $\|X\|_2$. Denote the Frobenius norm of $X$ as $\|X\|_F$. For a vector $v$, denote the Euclidean norm of $v$ as $\|v\|$.

Let $\tilde{\mathcal{D}}_t = \{x_1^{(t)}, x_2^{(t)}, \dots, x_N^{(t)}\}$ be $N$ i.i.d. samples of $\mathcal{D}_t$. Let $\sigma_1, \sigma_2, \dots, \sigma_N$ be independent Rademacher random variables. Denote the Rademacher complexity of task $t$ with $N$ samples from $\mathcal{D}_t$ as:

$$\mathcal{R}_N(\mathcal{F}) = \mathop{\mathbb{E}}_{\tilde{\mathcal{D}}_t, \sigma}\left[\sup_{f \in \mathcal{F}} \frac{1}{N} \sum_{i=1}^{N} \sigma_i f\left(x_i^{(t)}\right)\right]. \tag{7}$$

## A.1 Proof of Theorem 2.1

We prove the convergence rate of task modeling as a function of $n$—the number of subsets that one needs to sample in order to learn a task model, and $N$—the size of the target task's validation set used to evaluate $f_t$. Let $\boldsymbol{I} \in \mathbb{R}^{|\mathcal{S}| \times k}$ be a zero-one matrix including $\mathbb{1}_T$ as its row vectors, for all $T \in \mathcal{S}$. Let $\boldsymbol{f}$ be an $|\mathcal{S}|$ dimensional vector such that $\boldsymbol{f}_T = f_t(T)$ for every $T \in \mathcal{S}$. Let $\mathcal{I}_n \in \mathbb{R}^{n \times k}$ be a zero-one matrix including $\mathbb{1}_{S_1}, \dots, \mathbb{1}_{S_n}$ as its row vectors. Let $\hat{f}$ be an $n$ dimensional vector such that $\hat{f}_i = f_t(S_i)$.

Recall from equation (29) that the minimizer of the empirical loss $\hat{\mathcal{L}}_n(\theta)$ is equal to:[1]

$$\hat{\theta}_n = \left(\mathcal{I}_n^\top \mathcal{I}_n\right)^{-1} v_n,$$

where the $i$-th entry of $v_n$ is defined as

$$\sum_{1 \le j \le n:\, i \in S_j} f_t(S_j).$$

In a similar vein, denote the minimizer of the population loss $\mathcal{L}(\theta)$ as

$$\theta^\star = \left(\boldsymbol{I}^\top \boldsymbol{I}\right)^{-1} \boldsymbol{I}^\top \mathbb{E}\left[\boldsymbol{f}\right].$$

**Lemma A.1.** *In the setting of Theorem 2.1, let $\hat{\theta}_{|\mathcal{S}|}$ be defined as $\left(\frac{\boldsymbol{I}^\top \boldsymbol{I}}{|\mathcal{S}|}\right)^{-1} \frac{\boldsymbol{I}^\top \boldsymbol{f}}{|\mathcal{S}|}$. Conditional on $f_t$ and $\hat{\mathcal{D}}_1, \dots, \hat{\mathcal{D}}_k$, with probability $1 - 2\delta$ over the randomness of the sampled subsets $S_1, S_2, \dots, S_n$, for any $\delta \ge 0$, $\hat{\theta}_n$ converges to $\hat{\theta}_{|\mathcal{S}|}$ in probability:*

$$\left\|\hat{\theta}_n - \hat{\theta}_{|\mathcal{S}|}\right\| \le Z \sqrt{\frac{k}{n}}. \tag{8}$$

*where $Z = 4C\alpha^2 \log(2k\delta^{-1}) + (1 - \alpha/k)^{-3} C\alpha\delta^{-1/2}$.*

*Proof.* We will use the triangle inequality to attribute the error between $\hat{\theta}_n$ and $\hat{\theta}_{|\mathcal{S}|}$ to two parts.

$$\begin{aligned}
\left\|\hat{\theta}_n - \hat{\theta}_{|\mathcal{S}|}\right\| &= \left\|\left(\left(\frac{\mathcal{I}_n^\top \mathcal{I}_n}{n}\right)^{-1} - \left(\frac{\boldsymbol{I}^\top \boldsymbol{I}}{|\mathcal{S}|}\right)^{-1}\right) \frac{v_n}{n} + \left(\frac{\boldsymbol{I}^\top \boldsymbol{I}}{|\mathcal{S}|}\right)^{-1} \left(\frac{v_n}{n} - \frac{\boldsymbol{I}^\top \mathbb{E}\left[\boldsymbol{f}\right]}{|\mathcal{S}|}\right)\right\| \\
&\le \left\|\left(\frac{\mathcal{I}_n^\top \mathcal{I}_n}{n}\right)^{-1} - \left(\frac{\boldsymbol{I}^\top \boldsymbol{I}}{|\mathcal{S}|}\right)^{-1}\right\|_2 \cdot \left\|\frac{v_n}{n}\right\| & (9) \\
&+ \left\|\left(\frac{\boldsymbol{I}^\top \boldsymbol{I}}{|\mathcal{S}|}\right)^{-1}\right\|_2 \cdot \left\|\frac{v_n}{n} - \frac{\boldsymbol{I}^\top \boldsymbol{f}}{|\mathcal{S}|}\right\|. & (10)
\end{aligned}$$

We compare the sampled score vector $\frac{v_n}{n}$ and the population score vector $\frac{\boldsymbol{I}^\top \boldsymbol{f}}{|\mathcal{S}|}$. Recall that both vectors have $k$ coordinates, each corresponding to one task. For any task $i = 1, \dots, k$, let $\mathcal{E}_i$ denote the difference between the $i$-th coordinate of $\frac{v_n}{n}$ and the $i$-th coordinate of $\frac{\boldsymbol{I}^\top \boldsymbol{f}}{|\mathcal{S}|}$:

$$\mathcal{E}_i = \frac{1}{n} \sum_{1 \le j \le n:\ i \in S_j} f_t(S_j) - \frac{1}{|\mathcal{S}|} \sum_{T \in \mathcal{S}:\ i \in T} f_t(T). \tag{11}$$

[1] With a similar analysis one could also prove the convergence from $\hat{\mathcal{L}}_n(\cdot)$ to $\mathcal{L}(\cdot)$ with the minimizer of the ridge regression, which includes $\lambda$ times an identity matrix in the inverted sample covariance of $\hat{\theta}_n$.

Notice that the sampling of $S_1, S_2, \ldots, S_n$ is independent of the randomness in $f_{\mathcal{A}}$. Therefore, we have that the expectation of $\mathcal{E}_i$ is zero: $\mathbb{E}\left[\mathcal{E}_i\right] = 0$. Next, we apply the Chebyshev's inequality to analyze the deviation of $\mathcal{E}_i$ from its expectation. We consider the variance of $\mathcal{E}_i$, which is the expectation of $\mathcal{E}_i^2$:

$$\begin{aligned}\mathbb{E}\left[\mathcal{E}_i^2\right] &= \mathbb{E}\left[\left(\frac{1}{n}\sum_{1\le j\le n: i\in S_j} f_t(S_j) - \frac{1}{|\mathcal{S}|}\sum_{T\in\mathcal{S}: i\in T} f_t(T)\right)^2\right] \\ &= \mathbb{E}\left[\left(\sum_{1\le j\le n: i\in S_j} f_t(S_j)\right)^2 - \frac{2}{n\,|\mathcal{S}|}\sum_{1\le j\le n: i\in S_j} f_t(S_j)\sum_{T\in\mathcal{S}: i\in T} f_t(T) + \frac{1}{|\mathcal{S}|^2}\Big(\sum_{T\in\mathcal{S}: i\in T} f_t(T)\Big)^2\right] \end{aligned} \tag{12}$$

Notice that for any $T \in \mathcal{S}$ such that $i \in T$, the probability that $T$ is sampled in a size $n$ (training) set is equal to

$$\frac{\binom{|\mathcal{S}|-1}{n-1}}{\binom{|\mathcal{S}|}{n}} = \frac{n}{|\mathcal{S}|}.$$

For any two subsets $T \neq T'$, both in $\mathcal{S}$, such that $i \in T$ and $i \in T'$, the probability that $T$ and $T'$ are both sampled in a size $n$ (training) set is equal to

$$\frac{\binom{|\mathcal{S}|-1}{n-1}}{\binom{|\mathcal{S}|}{n}} \cdot \frac{\binom{|\mathcal{S}|-1}{n-1}}{\binom{|\mathcal{S}|}{n}} = \frac{n^2}{|\mathcal{S}|^2}.$$

Thus, by taking the expectation over the randomness of the sampled subsets in equation (12) conditional on $f_t$, we get that

$$\mathbb{E}\left[\mathcal{E}_i^2\right] = \mathbb{E}\left[\Big(\frac{1}{n\,|\mathcal{S}|} - \frac{1}{|\mathcal{S}|^2}\Big)\sum_{T\in\mathcal{S}: i\in T}\big(f_t(T)\big)^2\right] \le \frac{C^2}{n},$$

since we have assumed that the loss function $\ell(\cdot,\cdot)$ is bounded from above by an absolute constant $C$ and $f_t$ is the average loss. Therefore,

$$\mathbb{E}\left[\sum_{i=1}^{k}\mathcal{E}_i^2\right] \le \frac{C^2 k}{n}.$$

By Markov's inequality, for any $a > 0$,

$$\Pr\left[\sqrt{\sum_{i=1}^{k}\mathcal{E}_i^2} \ge a\sqrt{\frac{k}{n}}\right] \le \frac{C^2}{a^2}.$$

Therefore, with probability $1 - \delta$, for any $\delta > 0$, we have that

$$\left\|\frac{v_n}{n} - \frac{\boldsymbol{I}^\top\,\mathbb{E}\left[\boldsymbol{f}\right]}{|\mathcal{S}|}\right\| \le C\delta^{-1/2}\sqrt{\frac{k}{n}}. \tag{13}$$

Next, we use random matrix concentration results to analyze the difference between the indicator matrix of the sampled subsets and the indicator matrix of all subsets in $\mathcal{S}$. Denote by

$$E = \frac{\mathcal{I}_n^\top \mathcal{I}_n}{n} - \frac{\boldsymbol{I}^\top\boldsymbol{I}}{|\mathcal{S}|} \quad\text{and}\quad A = \frac{\boldsymbol{I}^\top\boldsymbol{I}}{\mathcal{S}}.$$

By the Sherman-Morrison formula (for matrix inversion), we get

$$\begin{aligned}\left\|\Big(\frac{\mathcal{I}_n^\top\mathcal{I}_n}{n}\Big)^{-1} - \Big(\frac{\boldsymbol{I}^\top\boldsymbol{I}}{|\mathcal{S}|}\Big)^{-1}\right\|_2 &= \left\|(E+A)^{-1} - A^{-1}\right\|_2 \\ &= A^{-1}\Big(AE^{-1} + \mathrm{Id}_{k\times k}\Big)^{-1} \\ &= A^{-1}E\Big(A+E\Big)^{-1} \\ &\le \big(\lambda_{\min}(A)\big)^{-1}\cdot\|E\|_2\cdot\big(\lambda_{\min}(A+E)^{-1}\big) \\ &\le \frac{\|E\|_2}{\lambda_{\min}(A)(\lambda_{\min}(A) - \|E\|_2)}. \end{aligned} \tag{14}$$

We now use the matrix Bernstein inequality (cf. Theorem 6.1.1 in Tropp [43]) to deal with the spectral norm of $E$. Let

$$X_i = \mathbb{1}_{S_i}\mathbb{1}_{S_i}^\top - \frac{\boldsymbol{\mathcal{I}}^\top \boldsymbol{\mathcal{I}}}{|\mathcal{S}|}, \text{ for any } i = 1, \dots, n.$$

Let $\mathcal{D}$ denote the uniform distribution over $\mathcal{S}$. In expectation over $\mathcal{D}$, we know that $\mathbb{E}[X_i] = 0$, for any $i = 1, \dots, n$. Additionally, $\|X_i\|_2 \le 2\alpha$, since it is a linear combination of indicator vectors with $\alpha$ ones. Therefore, for all $t \ge 0$,

$$\Pr\left[\|E\|_2 \ge t\right] = \Pr\left[\left\|\sum_{i=1}^n X_i\right\|_2 \ge nt\right] \le 2k \cdot \exp\left(-\frac{(nt)^2/2}{(2\alpha)^2 n + (2\alpha)nt/3}\right).$$

This implies (with some calculation) that for any $\delta \ge 0$, with probability at least $1 - \delta$,

$$\|E\|_2 \le \frac{4\alpha \cdot \log\left(2k\delta^{-1}\right)}{\sqrt{n}}. \tag{15}$$

By applying equation (13) into equation (9) and equation (15) into equation (10), we have shown that with probability at least $1 - 2\delta$, for any $\delta \ge 0$,

$$\left\|\hat{\theta}_n - \hat{\theta}_{|\mathcal{S}|}\right\| \le \left\|\frac{v_n}{n}\right\|_2 \cdot \frac{4\alpha \cdot \log\left(2k\delta^{-1}\right)}{\sqrt{n}} + \frac{1}{\left(\lambda_{\min}(A)\right)^2\left(\lambda_{\min}(A) - \|E\|_2\right)} \cdot C\delta^{-1/2}\sqrt{\frac{k}{n}}. \tag{16}$$

For the first part, let $z_i$ be the number of subsets $S_j$ among $1 \le j \le n$ such that $i \in S_j$, for any $i = 1, \dots, n$. Recall that the loss $\ell(\cdot, \cdot)$ is bounded from above by an absolute constant $C$. Thus,

$$\left\|\frac{v_n}{n}\right\| \le \frac{1}{n}\sqrt{C^2 \cdot \sum_{i=1}^k z_i^2} \le \frac{C}{n}\left(\sum_{i=1}^k z_i\right) = C\alpha. \tag{17}$$

Regarding the minimum eigenvalue of $A$, notice that the diagonal entry of $\frac{\boldsymbol{\mathcal{I}}^\top \boldsymbol{\mathcal{I}}}{|\mathcal{S}|}$ is equal to $\binom{k-1}{\alpha-1}$. The off diagonal entries of this matrix is equal to $\binom{k-2}{\alpha-2}$. Thus,

$$\lambda_{\min}(A) \ge 1 - \frac{\binom{k-2}{\alpha-2}}{\binom{k-1}{\alpha-1}} = 1 - \frac{\alpha - 1}{k - 1} \ge 1 - \frac{\alpha}{k}. \tag{18}$$

Applying equations (17) and (18) back into equation (16), we conclude that with probability at least $1 - 2\delta$, $\hat{\theta}_n$ deviates from $\hat{\theta}_{|\mathcal{S}|}$ by a rate of $\sqrt{k/n}$:

$$\left\|\hat{\theta}_n - \hat{\theta}_{|\mathcal{S}|}\right\| \le \left(4C\alpha^2 \log(2k\delta^{-1}) + (1 - \alpha/k)^{-3} C\alpha\delta^{-1/2}\right)\sqrt{\frac{k}{n}}.$$

□

Next, we show the uniform convergence of $\hat{\theta}_{|\mathcal{S}|}$. The key observation is that the size of $\mathcal{S}$ only depends on the number of tasks $k$. Therefore, one can afford to apply a union bound over $\mathcal{S}$.

**Lemma A.2.** *In the setting of Theorem 2.1, for any $\delta > 0$, with probability at least $1 - \delta$, the deviation between $\hat{\theta}_{|\mathcal{S}|}$ and $\theta^\star$ satisfies:*

$$\left\|\hat{\theta}_{|\mathcal{S}|} - \theta^\star\right\| \le (1 - \alpha/k)^{-1}\frac{\mathcal{R}_N(\mathcal{F})}{2} + (1 - \alpha/k)^{-1}\sqrt{\frac{\alpha \log\left(k/\delta\right)}{2N}}. \tag{19}$$

*Proof.* Based on the definitions of $\hat{\theta}_{|\mathcal{S}|}$ and $\theta^\star$, we analyze their difference as follows:

$$\begin{aligned}
\left\|\hat{\theta}_{|\mathcal{S}|} - \theta^\star\right\| &= \left\|\left(\boldsymbol{\mathcal{I}}^\top \boldsymbol{\mathcal{I}}\right)^{-1} \boldsymbol{\mathcal{I}}^\top \left(\boldsymbol{f} - \mathbb{E}\left[\boldsymbol{f}\right]\right)\right\| & (20)\\
&\le \left\|\sqrt{|\mathcal{S}|}\left(\boldsymbol{\mathcal{I}}^\top \boldsymbol{\mathcal{I}}\right)^{-1} \boldsymbol{\mathcal{I}}^\top\right\|_2 \cdot \frac{\|\boldsymbol{f} - \mathbb{E}\left[\boldsymbol{f}\right]\|}{\sqrt{|\mathcal{S}|}} \\
&= \left(\lambda_{\min}(\boldsymbol{\mathcal{I}}^\top \boldsymbol{\mathcal{I}})\right)^{-1/2} \cdot \frac{\|\boldsymbol{f} - \mathbb{E}\left[\boldsymbol{f}\right]\|}{\sqrt{|\mathcal{S}|}} \\
&\le (1 - \alpha)^{-1} \frac{\|\boldsymbol{f} - \mathbb{E}\left[\boldsymbol{f}\right]\|}{\sqrt{|\mathcal{S}|}}. & \text{(by equation (18))}
\end{aligned}$$

For each subset $T \in \mathcal{S}$, we will apply a Rademacher complexity based generalization bound to analyze the generalization error $\boldsymbol{f}_T - \mathbb{E}\left[\boldsymbol{f}_T\right]$. Recall the Rademacher complexity of $\mathcal{F}$ with $N_t$ samples from $\mathcal{D}_t$ is defined as

$$\mathcal{R}_N(\mathcal{F}) = \mathop{\mathbb{E}}_{\tilde{\mathcal{D}}_t,\sigma}\left[\sup_{f\in\mathcal{F}} \frac{1}{N}\sum_{j=1}^{N} \sigma_j f(x_j^{(t)})\right].$$

By Theorem 5 of Bartlett and Mendelson [5], with probability at least $1-\delta$, we can get:

$$\boldsymbol{f}_T \le \mathbb{E}\left[\boldsymbol{f}_T\right] + \frac{\mathcal{R}_N(\mathcal{F})}{2} + \sqrt{\frac{\log\left(1/\delta\right)}{2N}}. \tag{21}$$

Similarly, one can get the result for other direction of the error estimate. With a union bound over all subsets $T \in \mathcal{S}$, with probability at least $1-\delta$, we get:

$$\boldsymbol{f}_T \le \mathbb{E}\left[\boldsymbol{f}_T\right] + \frac{\mathcal{R}_N(\mathcal{F})}{2} + \sqrt{\frac{\alpha\log\left(k/\delta\right)}{2N}},\ \text{for all } T \in \mathcal{S}, \tag{22}$$

since $\log\left(\binom{k}{\alpha}/\delta\right) \le \alpha\log(k\delta^{-1})$. Let $z = \sqrt{\alpha\log\left(k\delta^{-1}\right)/(2N)}$. Applying equation (22) back into equation (20), we have shown

$$\begin{aligned}\left\|\hat{\theta}_{|\mathcal{S}|} - \theta^\star\right\| &\le (1-\alpha)^{-1}\sqrt{\frac{1}{|\mathcal{S}|}\sum_{T\in\mathcal{S}}\left(\frac{\mathcal{R}_N(\mathcal{F})}{2} + z\right)^2} \\ &= (1-\alpha)^{-1}\left(\frac{\mathcal{R}_N(\mathcal{F})}{2} + z\right).\end{aligned}$$

Thus, the proof is complete. □

Based on the result from Lemma A.1 and Lemma A.2, we are now ready to prove our main result.

*Proof of Theorem 2.1.* Notice that equation (4) follows by combining equation (8) (from Lemma A.1) and equation (19) (from Lemma A.2), together with the condition that $\alpha \le 1/2$.

To analyze the generalization error of $\hat{\mathcal{L}}_n(\hat{\theta}_n)$, we first expand it out as

$$\begin{aligned}\hat{\mathcal{L}}_n(\hat{\theta}_n) &= \left\|\mathcal{I}_n\hat{\theta}_n - \hat{f}\right\|^2 \\ &= \frac{1}{n}\left\|\mathcal{I}_n\hat{\theta}_n - \mathop{\mathbb{E}}_{\hat{f}}\left[\hat{f}\right] + \mathop{\mathbb{E}}_{\hat{f}}\left[\hat{f}\right] - \hat{f}\right\|^2 \\ &= \frac{1}{n}\left\|\mathcal{I}_n\hat{\theta}_n - \mathop{\mathbb{E}}_{\hat{f}}\left[\hat{f}\right]\right\|^2 + \frac{1}{n}\langle\mathcal{I}_n\hat{\theta}_n - \mathop{\mathbb{E}}_{\hat{f}}\left[\hat{f}\right], \mathop{\mathbb{E}}_{\hat{f}}\left[\hat{f}\right] - \hat{f}\rangle + \frac{1}{n}\left\|\mathop{\mathbb{E}}_{\hat{f}}\left[\hat{f}\right] - \hat{f}\right\|^2.\end{aligned} \tag{23}$$

Based on Lemma A.1, the distance between $\hat{\theta}_n$ and $\theta^\star$ is at the order of $O\left(n^{-1/2}\right)$ with high probability. We will use this result to deal with the first term in equation (23):

$$\begin{aligned}&\frac{1}{n}\left\|\mathcal{I}_n\hat{\theta}_n - \mathop{\mathbb{E}}_{\hat{f}}\left[\hat{f}\right]\right\|^2 - \frac{1}{n}\left\|\mathcal{I}_n\theta^\star - \mathop{\mathbb{E}}_{\hat{f}}\left[\hat{f}\right]\right\| && (24)\\ =&\left|\frac{1}{n}\langle\mathcal{I}_n^\top\mathcal{I}_n, \hat{\theta}_n(\hat{\theta}_n)^\top - \theta^\star(\theta^\star)^\top\rangle - \frac{2}{n}\langle\mathop{\mathbb{E}}_{\hat{f}}\left[\hat{f}\right], \hat{\theta}_n - \theta^\star\rangle\right| \\ \le&\left\|\frac{1}{n}\mathcal{I}_n^\top\mathcal{I}_n\right\|_2 \cdot \left\|\theta^\star(\theta^\star)^\top - \hat{\theta}_n(\hat{\theta}_n)^\top\right\|_F + \frac{2}{n}\left\|\mathop{\mathbb{E}}_{\hat{f}}\left[\hat{f}\right]\right\| \cdot \left\|\theta^\star - \hat{\theta}_n\right\| && \text{(by triangle inequality)}\\ \le&\alpha\left\|\theta^\star(\theta^\star)^\top - \hat{\theta}_n(\hat{\theta}_n)^\top\right\|_F + 2C\alpha\cdot e_1, && \text{(by equations (17) and (4))}\end{aligned}$$

where $e_1$ denotes the right hand side of equation (4). In the last step, we used the fact that $\mathcal{I}_n^\top \mathcal{I}_n / n$ is the average of $n$ rank one matrices, each with spectral norm $\alpha$, since they have exactly $\alpha$ ones. Next,

$$\begin{aligned}
\left\|\theta^\star(\theta^\star)^\top - \hat{\theta}_n(\hat{\theta}_n)^\top\right\|_F &= \left\|\theta^\star(\theta^\star - \hat{\theta}_n)^\top + (\theta^\star - \hat{\theta}_n)(\hat{\theta}_n)^\top\right\|_F \\
&\le \left\|\theta^\star(\theta^\star - \hat{\theta}_n)^\top\right\|_F + \left\|(\theta^\star - \hat{\theta}_n)(\hat{\theta}_n)^\top\right\|_F && \text{(by triangle inequality)} \\
&\le \left(\left\|\theta^\star\right\| + \left\|\hat{\theta}_n\right\|\right) e_1. && \text{(by equation (4))}
\end{aligned}$$

We show that the norm of $\theta^\star$ and $\hat{\theta}_n$ are both bounded by a constant factor times $\sqrt{k}$. To see this,

$$\begin{aligned}
\left\|\theta^\star\right\| &= \left\|(\boldsymbol{\mathcal{I}}^\top \boldsymbol{\mathcal{I}})^{-1}\boldsymbol{\mathcal{I}}^\top \mathop{\mathbb{E}}_{\boldsymbol{f}}[\boldsymbol{f}]\right\| \\
&\le \left\|\left(\frac{\boldsymbol{\mathcal{I}}^\top \boldsymbol{\mathcal{I}}}{|\mathcal{S}|}\right)^{-1}\right\|_2 \cdot \left\|\frac{\boldsymbol{\mathcal{I}}^\top \mathbb{E}_{\boldsymbol{f}}[\boldsymbol{f}]}{|\mathcal{S}|}\right\| \\
&\le (1-\alpha/k)^{-1} \cdot C\sqrt{\alpha} && \text{(by equation (18) and } \ell(\cdot,\cdot) \le C\text{)}
\end{aligned}$$

Notice that the spectral norm between $\boldsymbol{\mathcal{I}}^\top \boldsymbol{\mathcal{I}} / |\mathcal{S}|$ and $\mathcal{I}_n^\top \mathcal{I}_n / n$ is bounded by equation (15). Thus, with similar steps as above, we can show

$$\left\|\hat{\theta}_n\right\| \le \left((1-\alpha/k)^{-1} + \frac{4\alpha \log\left(2k\delta^{-1}\right)}{\sqrt{n}}\right) C\sqrt{k}.$$

To wrap up our analysis above, we have shown that equation (24) is at most

$$e_3 = \alpha\left(2(1-\alpha/k)^{-1} + \frac{4\alpha\log\left(2k\delta^{-1}\right)}{\sqrt{n}}\right) C\sqrt{\alpha}\cdot e_1 + 2C\alpha \cdot e_1.$$

Next, we consider the second term in equation (23). Let $e_2$ be the deviation error indicated in equation (22) Thus, every entry of $\hat{f} - \mathbb{E}_{\hat{f}}\left[\hat{f}\right]$ is at most $e_2$. Besides, each entry of $\mathcal{I}_n \hat{\theta}_n - \mathbb{E}_{\hat{f}}\left[\hat{f}\right]$ is less than

$$\sqrt{\alpha}\|\hat{\theta}_n\| + C.$$

Thus, the second term in equation (23) is less than

$$e_4 = e_2\left(\sqrt{\alpha}\left((1-\alpha/k)^{-1} + \frac{4\alpha\log\left(2k\delta^{-1}\right)}{\sqrt{n}}\right)C\sqrt{\alpha} + C\right)$$

For the population loss $\mathcal{L}(\theta^\star)$, notice that

$$\begin{aligned}
\mathcal{L}(\theta^\star) &= \mathop{\mathbb{E}}_{\boldsymbol{f}}\left[\frac{1}{|\mathcal{S}|}\left\|\boldsymbol{\mathcal{I}}\theta^\star - \boldsymbol{f}\right\|^2\right] \\
&= \mathop{\mathbb{E}}_{\boldsymbol{f}}\left[\frac{1}{|\mathcal{S}|}\left\|\boldsymbol{\mathcal{I}}\theta^\star - \mathop{\mathbb{E}}_{\boldsymbol{f}}[\boldsymbol{f}] + \mathop{\mathbb{E}}_{\boldsymbol{f}}[\boldsymbol{f}] - \boldsymbol{f}\right\|^2\right] \\
&= \frac{1}{|\mathcal{S}|}\left\|\boldsymbol{\mathcal{I}}\theta^\star - \mathop{\mathbb{E}}_{\boldsymbol{f}}[\boldsymbol{f}]\right\|^2 + \frac{1}{|\mathcal{S}|}\left(\mathop{\mathbb{E}}_{\boldsymbol{f}}\left[\left\|\boldsymbol{f} - \mathop{\mathbb{E}}_{\boldsymbol{f}}[\boldsymbol{f}]\right\|^2\right]\right) \qquad (25)
\end{aligned}$$

We know that each entry of $\boldsymbol{\mathcal{I}}\theta^\star - \mathbb{E}_{\boldsymbol{f}}[\boldsymbol{f}]$ is at most $(1-\alpha/k)^{-1}\sqrt{\alpha} + C$. Thus, by Hoeffding's inequality, with probability at least $1-\delta$, we have

$$\left|\frac{1}{n}\left\|\mathcal{I}_n\theta^\star - \mathop{\mathbb{E}}_{\hat{f}}\left[\hat{f}\right]\right\| - \frac{1}{|\mathcal{S}|}\left\|\boldsymbol{\mathcal{I}}\theta^\star - \mathop{\mathbb{E}}_{\boldsymbol{f}}[\boldsymbol{f}]\right\|\right| \le \left((1-\alpha/k)^{-1}\sqrt{\alpha} + C\right)\sqrt{\frac{\log\left(\delta^{-1}\right)}{n}}. \qquad (26)$$

Lastly, we consider the third term in equation (23), compared with the second term in equation (25). For every $T \in \mathcal{S}$, let $e_T = \boldsymbol{f}_T - \mathbb{E}[\boldsymbol{f}_T]$. By equation (22), we know that $e_T$ is of order $O(N^{-1/2})$, for every $T \in \mathcal{S}$. Therefore

$$\left|\frac{1}{n}\sum_{i=1}^{n} e_{S_i}^2\right| \le \left(\frac{\mathcal{R}_N(\mathcal{F})}{2} + \sqrt{\frac{\alpha\log(k/\delta)}{2N}}\right)^2, \qquad (27)$$

which is of order $O(N^{-1})$. Similarly, the same holds for variance of $\boldsymbol{f}$ in the second term of equation (25). Comparing equations (26) and (23), we have shown that

$$\begin{aligned}\mathcal{L}(\theta^\star) - \hat{\mathcal{L}}_n(\hat{\theta}_n) &\le \left((1-\alpha/k)^{-1}\sqrt{\alpha} + C + C^2\right)\sqrt{\frac{\log(\delta^{-1})}{n}} + C \cdot e_2 + e_3 + e_4 \\ &\lesssim (C + C\alpha)\left(\mathcal{R}_N(\mathcal{F}) + \frac{\sqrt{\alpha \log(k\delta^{-1})}}{\sqrt{N}}\right) + \frac{C^2\alpha^{7/2}\log\left(2k\delta^{-1}\right) + 8C^2\alpha^{5/2}\delta^{-1/2}\sqrt{k}}{\sqrt{n}}.\end{aligned}$$

The above follows by incorporating the definitions of the error terms. Thus, we have completed the proof of equation (5). The proof is now finished. □

## A.2 Proof of Theorem 2.2

Recall that $\mathcal{I}_n \in \{0,1\}^{n\times k}$ is the indicator matrix corresponding to the task indices from the training dataset. Given a set of tasks $S$ with size $\alpha$, denote their feature covariate matrices and label vectors as $(X_1, Y_1), (X_2, Y_2), \dots, (X_\alpha, Y_\alpha)$. With hard parameter sharing [51], we minimize

$$\ell(B) = \sum_{i=1}^{\alpha} \|X_i B - Y_i\|^2. \tag{28}$$

The minimizer of $\ell(B)$, denoted as $\hat{B}$, is equal to the following

$$\hat{B} = \left(\sum_{i=1}^{\alpha} X_i^\top X_i\right)^{-1} \left(\sum_{i=1}^{\alpha} X_i^\top Y_i\right).$$

For isotropic covariates, the loss of using $B$ on the validation set of the target task is equal to

$$f_t(S) = \left\|\hat{B} - \beta^{(t)}\right\|^2 + O\left(\sqrt{\frac{p}{N}}\right).$$

By solving equation (2), the estimated task model $\hat{\theta}_n$ is equal to

$$\hat{\theta}_n = \left(\mathcal{I}_n^\top \mathcal{I}_n\right)^{-1} v_n, \tag{29}$$

where $v_n = \mathcal{I}_n^\top \hat{f} \in \mathbb{R}^k$ is a vector that satisfies:

$$v_n(i) = \sum_{j:\, i \in \mathcal{S}_j} f_t(S_j), \text{ for any } 1 \le i \le k.$$

First we show that $\hat{\theta}_n$ is approximately a scaling of the vector $v_n$. The key observation is that $\mathcal{I}_n^\top \mathcal{I}_n$ is approximately an identity matrix plus a constant shift for every task.

**Lemma A.3.** *In the setting of Theorem 2.2, with probability $1-\delta$, for any $\delta > 0$, the following holds:*

$$\left|\frac{\hat{\theta}_n(i) - \hat{\theta}_n(j)}{n} - \frac{k}{\alpha} \cdot \frac{v_n(i) - v_n(j)}{n}\right| \lesssim \frac{\log(\delta^{-1}k)}{\sqrt{n}}, \text{ for any } 1 \le i < j \le k. \tag{30}$$

*Proof.* we have that $Y_i = X_i\beta^{(i)} + \epsilon^{(i)}$, where $\epsilon^{(i)}$ is a random vector whose entries are sampled independently with mean 0 and variance $\sigma^2$. We have

$$f_t(S) = \left\|\left(\sum_{i=1}^{\alpha} X_i^\top X_i\right)^{-1} \sum_{i=1}^{\alpha} X_i^\top \epsilon^{(i)}\right\|^2. \tag{31}$$

For a task $i$, we know that its coefficient is equal to the $i$-th entry of

$$\left(\frac{\mathcal{I}_n^\top \mathcal{I}_n}{n}\right)^{-1} \frac{\mathcal{I}_n^\top \hat{f}}{n},$$

Let $Z = \mathcal{I}_n^\top \mathcal{I}_n / n$. The expectation of $Z$ over the randomness of $\mathcal{I}_n$ satisfies

$$\mathbb{E}\left[Z\right] = \frac{\alpha}{k}\,\mathrm{Id}_{k\times k} + \frac{\alpha(\alpha-1)}{k(k-1)} e e^\top,$$

where $e \in \mathbb{R}^k$ is the all ones vector. Thus, by the Woodbury matrix identity,

$$\mathop{\mathbb{E}}_{Z}\left[Z\right]^{-1} = \frac{k}{\alpha}\left(\mathrm{Id}_{k\times k} - \frac{k(\alpha-1)}{\alpha(k\alpha-1)}ee^\top\right). \tag{32}$$

Thus, for any $i \neq j$, we observe that

$$\begin{aligned}\left|\frac{\hat\theta_n(i)-\hat\theta_n(j)}{n} - \frac{k}{\alpha}\cdot\frac{v_n(i)-v_n(j)}{n}\right| &= \left|(e_i-e_j)^\top\left(Z^{-1}-\mathbb{E}\left[Z\right]^{-1}\right)\frac{v_n}{n}\right| \\ &\leq \|e_i-e_j\|\cdot\left\|Z^{-1}-\mathbb{E}\left[Z\right]^{-1}\right\|_2\cdot\left\|\frac{v_n}{n}\right\| \\ &\leq 2C\alpha\cdot\left\|Z^{-1}-\mathbb{E}\left[Z\right]^{-1}\right\|_2 && \text{(by equation (17))} \\ &\leq \frac{4\alpha\log\left(2k\delta^{-1}\right)}{\sqrt{n}}\frac{2}{(1-\alpha/k)^2}. && \text{(by equations (14), (15), (18))}\end{aligned}$$

The last step follows by applying equations (15) and (18) into equation (14). Thus, we have finished the proof of equation (30). □

Second we show that provided $n$ and $d$ are sufficiently large, a separation exists in $v_n$ between related and unrelated tasks.

*Proof of Theorem 2.2.* We calculate $v_n(i)/n$ for all $i = 1, \dots, k$ and compare it between a related task and an unrelated task. We first compare their expectations over the randomly sampled subsets. By equation (13), we get

$$\begin{aligned}\left|\frac{v_n(i)}{n} - \frac{1}{|\mathcal{S}|}\sum_{T\in\mathcal{S}:i\in T} f_t(T)\right| &\leq \frac{Ck\delta^{-1/2}}{\sqrt{n}}, \text{ and} \\ \left|\frac{v_n(j)}{n} - \frac{1}{|\mathcal{S}|}\sum_{T\in\mathcal{S}:j\in T} f_t(T)\right| &\leq \frac{Ck\delta^{-1/2}}{\sqrt{n}}.\end{aligned}$$

Therefore, by applying the triangle inequality with the above two results, we get

$$\left|\frac{v_n(i)-v_n(j)}{n} - \frac{\sum_{T\in\mathcal{S}:i\in T} f_t(T) - \sum_{T\in\mathcal{S}:j\in T} f_t(T)}{|\mathcal{S}|}\right| \leq \frac{2Ck\delta^{-1/2}}{\sqrt{n}}. \tag{33}$$

To deal with equation (33), we shall apply a union bound over the sample covariance of every subset $T$ in $\mathcal{S}$ to show that they are close to their expectation. By Gaussian covariance estimation results (e.g., equation (6.12) in Wainwright [46]), for a fixed $T \in \mathcal{S}$, we get

$$\left|\frac{1}{md}\sum_{j=1}^{m} X_{i_j}^\top X_{i_j} - \mathrm{Id}_{p\times p}\right| \leq 2\sqrt{\frac{p}{md}} + 2\epsilon + \left(\sqrt{\frac{p}{md}}+\epsilon\right)^2,$$

with probability at least $1-2\exp(-md\epsilon^2/2)$. With a union bound over all $T \in \mathcal{S}$, we have that the above holds with probability at least $1-\delta$ for all $T \in \mathcal{S}$, with $\epsilon = \sqrt{2\alpha k\log(2k\delta^{-1})/(md)}$. Let $\varepsilon_1$ denote the error term above:

$$\varepsilon_1 = 2\sqrt{\frac{p}{md}} + 2\sqrt{\frac{2\alpha\log(2k\delta^{-1})}{md}} + \left(\sqrt{\frac{p}{md}}+\epsilon\right)^2.$$

Let $u_T = \frac{1}{md}\sum_{j\in T} X_j^\top \varepsilon^{(j)}$, for any $T \in \mathcal{S}$. Therefore, , one can verify that

$$\left|f_t(T) - \|u_T\|^2\right| \leq \left((1-\varepsilon_1)^{-2}-1\right)\|u_T\|^2 \leq 3\varepsilon_1\|u_T\|^2.$$

Notice that

$$\mathbb{E}\left[\|u_T\|^2\right] = \mathbb{E}\left[\frac{1}{(md)^2}\,\mathrm{Tr}\left[\sum_{j\in T} X_j^\top \varepsilon^{(j)}(\varepsilon^{(j)})^\top X_j\right]\right].$$

If $j$ is a related task, then the expectation over $\varepsilon^{(j)}$ is equal to $a^2\,\mathrm{Id}$ by Assumption ??. If $j$ is an unrelated task, on the other hand, then the expectation over $\varepsilon^{(t)}$ is equal to $b^2\,\mathrm{Id}$. Let $s(T)$ be equal to the number of similar tasks in $T$. Thus,

$$\mathbb{E}\left[\|u_T\|^2\right] = \frac{p(a^2 s(T) + b^2(m-s(T)))}{m^2 d}.$$

To argue about the deviation error of $\|u_T\|^2$, we use the following two estimates (see, e.g., Vershynin [44]), which holds with high probability:

$$\left|(\varepsilon^{(j)})^\top X_j X_j^\top \varepsilon^{(j)} - \mathbb{E}\left[(\varepsilon^{(j)})^\top X_j X_j^\top \varepsilon^{(j)}\right]\right| \lesssim p\sqrt{d}a^2, \text{ for any } j = 1, \dots, k$$

$$\left|(\varepsilon^{(i)})^\top X_i X_j^\top \varepsilon^{(j)}\right| \lesssim p\sqrt{d}a^2, \text{ for any } 1 \le i < j \le k.$$

Therefore, we get that for any $T \in \mathcal{S}$,

$$\left|\|u_T\|^2 - \mathbb{E}\left[\|u_T\|^2\right]\right| \le \frac{p\sqrt{d}a^2}{d^2}.$$

To finish the proof, consider a related task $i$ versus an unrelated task $j$. Provided that

$$(1 - 3\varepsilon_1)\frac{p(a^2 - b^2)}{m^2 d} \ge (1 + 3\varepsilon_1)\frac{p\sqrt{d}a^2}{d^2} + \frac{2Ck\delta^{-1/2}}{\sqrt{n}}, \tag{34}$$

there must exist a threshold that separates all the related tasks from the unrelated tasks. One can verify that condition (34) is satisfied when

$$n \gtrsim C^2 \cdot k^2 \cdot \frac{1}{(a^2 - b^2)^2}, \text{ and } d \gtrsim \left(\frac{a^2}{a^2 - b^2}\right)^2 k^4 + k \log\left(\frac{2k}{\delta}\right) + p.$$

Set the threshold $\gamma$ as $k/\alpha$ times any value between the left and right hand side of equation (34). Thus, when $n$ and $d$ satisfy the condition above, combined with Lemma A.3, with high probability, for any $i$ such that $\hat{\theta}_n(i) < \gamma$, $i$ must be a related task. When $\hat{\theta}_n(j) > \gamma$, $i$ much be a unrelated task. Thus, we have finished the proof. □

# B Experiment Details

We describe details that were left out from the main text of the paper. First, we describe the additional experimental setup and the implementation specifics. Second, we present results to further validate the sample complexity of task modeling. Third, we provide the experimental results that are omitted from Section 3.

## B.1 Additional experimental setup

**Experimental setup for predicting higher-order transfers.** Figure 1 (Top) measures the accuracy of task modeling in predicting whether combining a set of source tasks $S$ with a primary target task leads to a positive transfer to the target task. We measure the positive transfer as whether training with the set of tasks $S$ improves single task learning of the target task. Figure 1 (Bottom) measures the correlation between multitask prediction losses $f_t(S)$ and task model predictions $g(S)$ as the size of subset $|S|$ varies. For previous approaches [18, 42], we use the higher-order approximation that averages first-order task affinity in a set $S$ as the prediction score $g(S)$. Both figures are studied on the target task HI with fifty source tasks.

Figure 2 measures the transferability from a source task to a target task in multitask learning. For each figure, we fix a target task and vary the source task. We measure the transferability as the difference between: (i) the multitask prediction result from a source and the target task averaged over multiple subsets containing the source task; (ii) single task learning with the target task alone. For both, we measure the worst-group accuracy of the target task.

Figure 3 (Top) provides the convergence of task modeling on binary prediction tasks. We use four target tasks, including HI, LA, MN, and NM. Figure 3 (Bottom) provides the convergence of task modeling on text datasets. We collect twenty-five tasks from several natural language processing benchmarks, including GLUE [48], SuperGLUE [47], TweetEval [3], and ANLI [30]. The collection spans numerous categories of tasks, including sentence classification, natural language inference, and question answering. Table 5 shows the statistics of the twenty-five tasks. We choose four target tasks, including STS-B, RTE, WNLI, and Emotion. We use BERT-Mini as the encoder. The encoder module is shared for all tasks, and a separate predictor is assigned for each task. We construct the task models using $n = 200$ sampled sets with $|S| = 5$ out of $k = 24$ source tasks. We construct a holdout set of size 50. We set the prediction loss $f_t$ as the loss of task $t$.

The abbreviation of each US state follows the convention. We include the ones we have referred to for reference: California (CA), Hawaii (HI), Kansas (KS), Louisiana (LA), Minnesota (MN), Nevada (NV), New Jersey (NJ), New Mexico (NM), Rhode Island (RI), and South Carolina (SC).

**Implementation details.** We report the results for baselines by running the official open-sourced implementations. We describe the hyperparameters for baselines as follows. For higher-order approximation [42] and task affinity grouping [18], we compute the task affinity scores between source tasks and target tasks. Then, we select $m$ source tasks as the tasks with the largest task affinity scores for each target task. $m$ is searched between 0 and the number of the source tasks. For gradient decomposition [14], we search the number of decomposition basis and auxiliary task gradient direction parameters, following the search space in [14]. For target-aware weighted training [12], we search the task weight learning rate in $[10^{-2}, 10^2]$. For our approach (cf. Algorithm 1), we use the threshold $\gamma$ in the range of $[-0.2, 0.2]$. The hyperparameters are tuned on the validation dataset by grid search. For each target task, we search 10 times over the hyperparameter space. We use the same number of trials in tuning hyperparameters for baselines.

Table 5: Dataset description and statistics of twenty-five text datasets.

| Task | Benchmark | Train. Set | Dev. Set | Task Category | Metrics |
|---|---|---|---|---|---|
| CoLA | GLUE | 8.5k | 1k | Grammar acceptability | Matthews corr. |
| MRPC | GLUE | 3.7k | 1.7k | Sentence Paraphrase | Acc./F1 |
| RTE | GLUE | 2.5k | 3k | Natural language inference | Acc. |
| SST-2 | GLUE | 67k | 1.8k | Sentence classification | Acc. |
| STS-B | GLUE | 7k | 1.4k | Sentence similarity | Pearson/Spearman corr. |
| WNLI | GLUE | 634 | 146 | Natural language inference | Acc. |
| BoolQ | SuperGLUE | 9.4k | 3.3k | Question answering | Acc. |
| CB | SuperGLUE | 250 | 57 | Natural language inference | Acc./F1 |
| COPA | SuperGLUE | 400 | 100 | Question answering | Acc. |
| MultiRC | SuperGLUE | 5.1k | 953 | Question answering | $\mathrm{F1}_a$/EM |
| WiC | SuperGLUE | 6k | 638 | Word sense disambiguation | Acc. |
| WSC | SuperGLUE | 554 | 104 | Coreference resolution | Acc. |
| Emoji | TweetEval | 45k | 5k | Sentence classification | Macro-averaged F1 |
| Emotion | TweetEval | 3.2k | 374 | Sentence classification | Macro-averaged F1 |
| Hate | TweetEval | 9k | 1k | Sentence classification | Macro-averaged F1 |
| Irony | TweetEval | 2.9k | 955 | Sentence classification | $\mathrm{F1}^{(i)}$ |
| Offensive | TweetEval | 12k | 1.3k | Sentence classification | Macro-averaged F1 |
| Sentiment | TweetEval | 45k | 2k | Sentence classification | Macro-averaged Recall |
| Stance (Abortion) | TweetEval | 587 | 66 | Sentence classification | Avg. of $\mathrm{F1}^{(a)}$ and $\mathrm{F1}^{(f)}$ |
| Stance (Atheism) | TweetEval | 461 | 52 | Sentence classification | Avg. of $\mathrm{F1}^{(a)}$ and $\mathrm{F1}^{(f)}$ |
| Stance (Climate) | TweetEval | 355 | 40 | Sentence classification | Avg. of $\mathrm{F1}^{(a)}$ and $\mathrm{F1}^{(f)}$ |
| Stance (Feminism) | TweetEval | 597 | 67 | Sentence classification | Avg. of $\mathrm{F1}^{(a)}$ and $\mathrm{F1}^{(f)}$ |
| Stance (H. Clinton) | TweetEval | 620 | 69 | Sentence classification | Avg. of $\mathrm{F1}^{(a)}$ and $\mathrm{F1}^{(f)}$ |
| ANLI (A1) | ANLI | 1.7k | 1k | Natural language inference | Acc. |
| ANLI (A2) | ANLI | 4.5k | 1k | Natural language inference | Acc. |

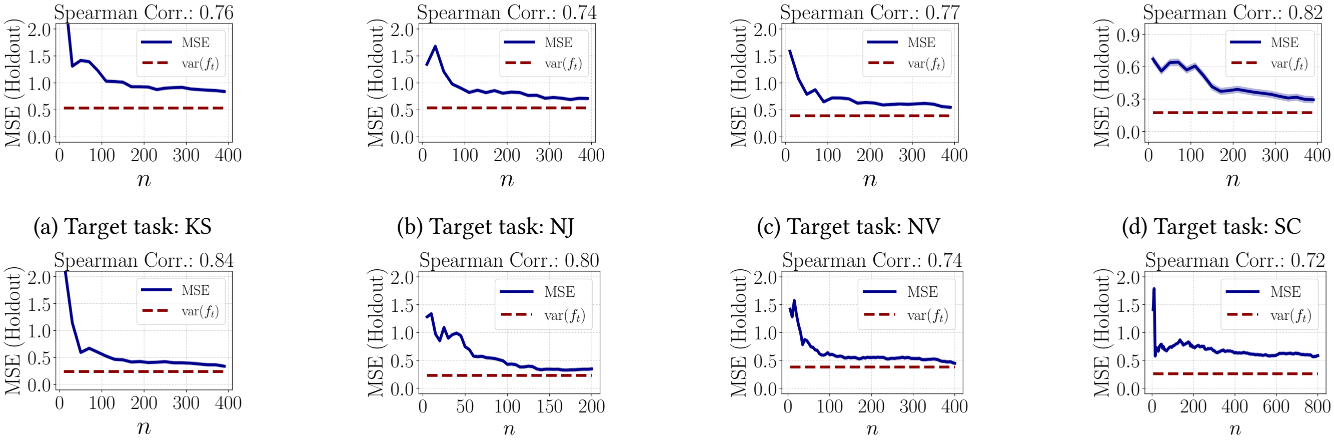

(a) Target task: KS

(b) Target task: NJ

(c) Target task: NV

(d) Target task: SC

(e) Target task: RI

(f) Target task: Chemprot

(g) Target task: TREC

(h) Target task: Semeval

Figure 5: The MSE of task modeling consistently converges close to the variance of $f_t$ for various tasks. **(a-e)** Binary classification tasks. **(f-h)** Text classification tasks with noisy supervision sources.

## B.2 Results on the convergence of task modeling

Section 2.2 presents that the sample complexity for task models to converge is nearly linear to the number of tasks. We further validate the convergence of task modeling on ten more target tasks, including five binary classification tasks and five text classification tasks with noisy supervision sources. We measure the MSE between task model predictions and empirically training results on the holdout set. The experimental setup of is described in Section 3.1. Figure 5 shows the results. We observe similar results as in Figure 3 that the MSE of task models consistently converges to the variance of the prediction loss. Hence, we conclude that the convergence of task modeling generally holds for various datasets.

Table 6: Comparison of different loss functions and exhaustive search over all subsets of at most two source tasks.

| | HI | KS | LA | NJ | NV | SC |
|---|---|---|---|---|---|---|
| Exhaustive search of $\lvert S \rvert \le 2$ | 75.10±0.37 | 77.03±0.76 | 73.60±1.02 | 77.40±0.24 | 73.21±1.10 | 77.16±0.21 |
| $f_t$ uses zero-one accuracy | 75.16±0.70 | 76.39±1.09 | 75.15±0.43 | 77.40±0.49 | 74.34±1.81 | 77.29±0.19 |
| $f_t$ uses cross-entropy loss | 75.33±0.80 | 75.82±0.60 | 74.19±1.37 | 77.51±0.35 | 74.55±1.60 | 77.21±0.27 |
| $f_t$ uses classification margin | 75.47±0.73 | 76.96±0.69 | 75.62±0.11 | 78.17±0.36 | 75.21±0.52 | 77.62±0.34 |

Table 7: Violation of two fairness measures (demographic parity and equality of opportunity) on six binary prediction tasks with tabular features, averaged over ten random seeds.

| Demographic parity | HI | KS | LA | NJ | NV | SC | Avg. Rank |
|---|---|---|---|---|---|---|---|
| Empirical risk minimization | 12.95±1.76 | 4.09±1.15 | 26.30±1.21 | 26.06±0.53 | 12.62±1.99 | 22.51±0.47 | 6.3 |
| Hard parameter sharing | 8.25±1.31 | 4.06±1.17 | 21.24±0.66 | 27.73±0.94 | 13.35±0.51 | 18.83±0.80 | 5.0 |
| Higher-order approx. [42] | 8.63±2.95 | 6.15±3.00 | 22.83±0.53 | 26.14±0.29 | 13.15±0.64 | 19.39±1.05 | 5.6 |
| Gradient similarity [18] | 9.39±1.45 | 3.26±1.21 | 20.61±0.55 | 25.51±1.17 | 12.50±1.10 | 18.91±0.92 | 3.5 |
| Task affinity grouping [18] | 8.93±2.35 | 3.97±0.61 | 20.72±0.86 | 25.21±0.68 | 12.24±0.82 | 18.77±0.85 | 2.8 |
| Weighted training [12] | 18.12±1.80 | 4.84±0.71 | 25.77±0.94 | 25.66±0.38 | 12.40±0.74 | 23.16±0.42 | 6.0 |
| Gradient decomposition [14] | 11.98±2.55 | 2.40±0.91 | 27.38±0.93 | 26.10±0.55 | 13.29±0.40 | 21.87±0.58 | 5.6 |
| **Task modeling (Alg. 1)** | **7.63±2.12** | **1.06±0.62** | **17.25±1.13** | **24.96±0.63** | **11.34±1.31** | **17.66±0.80** | **1.0** |
| Equality of opportunity | HI | KS | LA | NJ | NV | SC | |
| Empirical risk minimization | 9.86±1.29 | 1.43±3.62 | 29.64±3.24 | 22.43±1.02 | 13.61±3.67 | 29.93±0.77 | 6.0 |
| Hard parameter sharing | 3.86±0.84 | 2.03±2.11 | 21.26±1.35 | 24.43±1.49 | 12.14±2.21 | 21.22±1.75 | 5.0 |
| Higher-order approx. [42] | 3.55±2.85 | 4.34±3.18 | 22.88±1.72 | 22.98±1.18 | 12.92±2.23 | 23.31±1.77 | 5.3 |
| Gradient similarity [18] | 3.96±0.60 | 1.72±1.94 | 20.89±0.92 | **21.48±1.79** | 12.78±2.92 | 22.23±2.08 | 3.6 |
| Task affinity grouping [18] | 4.27±0.25 | 1.18±0.97 | 20.66±1.43 | 21.89±0.69 | 11.66±1.58 | 19.89±1.10 | 3.0 |
| Weighted training [12] | 4.21±2.25 | 1.40±2.14 | 30.38±2.17 | 23.26±0.30 | 11.77±1.01 | 30.86±0.84 | 5.6 |
| Gradient decomposition [14] | 3.18±4.92 | 6.01±2.47 | 32.31±0.86 | 22.83±1.01 | 15.48±1.17 | 29.81±1.19 | 6.1 |
| **Task modeling (Alg. 1)** | **0.24±1.32** | **0.21±1.34** | **14.14±2.32** | **21.48±0.90** | **9.65±3.49** | **18.54±1.61** | **1.0** |

### B.3 Omitted results from Section 3

**Results for improving fairness measures.** We show that task modeling is applicable to various performance metrics for capturing task affinity. Besides the average performance and worst-group performance discussed in Section 3.3, we consider two fairness measures: demographic parity and equal opportunity [15]. The demographic parity measure is defined as: $\lvert \Pr[\hat{y} = 1 \mid g = \text{black}] - \Pr[\hat{y} = 1 \mid g = \text{white}] \rvert$. This measures the difference of the positive rates between the white and African American demographic groups. The equality of opportunity measure is defined as: $\lvert \Pr[\hat{y} = 1 \mid y = 1, g = \text{black}] - \Pr[\hat{y} = 1 \mid y = 1, g = \text{white}] \rvert$. This measures the difference of the true positive rates between the two groups. We consider the binary classification tasks with multiple subpopulation groups. Table 7 shows the comparative results.

First, similar to the worst-group accuracy results, we find that multitask approaches (including ours and previous methods) decrease the violation of both fairness measures compared to ERM, suggesting the benefit of data augmentation. Second, our approach consistently reduces both fairness measure violations more by **1.26%** and **2.31%** on average than previous multitask learning approaches, respectively.

**Varying the number of sampled sets $n$.** We study how the number of sampled sets affect the selected task in the constructed task models. We measure the effect by comparing the 10 tasks with the smallest coefficients estimated from $n = 100, 200, 400$ subsets on two target tasks. We observe that using 100 and 200 subsets identifies 7 and 9 the same source tasks as using 400, respectively. Thus, we conclude that task selection results remain stable to the number of sampled sets.

We report the selected tasks with different numbers of sampled sets in the following. On target task HI, with 400 subsets, the ten tasks with the smallest task model coefficients are {CA NY TX FL PA IL OH NJ MI MA}. Using 200 subsets selects {CA NY TX FL PA IL OH NJ MI MA}. Using 100 subsets selects {CA TX NY PA OH FL NJ IL IN CO}. On target task LA, with 400 subsets, the ten tasks with the smallest task model coefficients are {CA TX NY FL IL GA PA MI NJ VA}. Using 200 subsets selects {CA TX NY FL IL PA NJ GA MI NC}. Using 100 subsets selects {CA NY TX FL IL NC GA IN CO PA}.

**Runtime results.** We report the GPU hours of contructing task models for each of the eleven target tasks in Table 3 and 4. Dataset (GPU hours) are listed in the following: Youtube (4.0), TREC (37.0), CDR (55.4), Chemprot (68.2), Semeval (85.9), HI (42.4), KS (44.0), LA (49.9), NJ (47.6), NV (43.7), SC (50.2).

# C Further Related Work Discussion

In the last section, we provide additional discussion of related work and connections to our work below, which is left from Section 1.1 due to space limit.

## C.1 Cross-task transfer learning

Learning from prior and related experiences is one of the hallmarks of human learning; thus, building new learning algorithms towards this end has vast potential for real-world applications [2]. Our work builds on a classical idea of learning a shared representation from multiple tasks to improve generalization for all tasks. As mentioned in Section 1.1, our problem setting focuses on the performance of a primary target task of interest. In the multitask learning literature, many works focus on the average performance of all tasks. It is conceivable that the task modeling approach can be adopted for this objective, too—this is a promising research question left for future work.

**Multitask representation learning.** A critical component of designing multitask learning algorithms and networks to encourage information transfer across different tasks. For example, learning a shared low-dimensional representation via dimension reduction is one way to restrict the model capacity to encourage positive transfer [7]. With convex optimization methods, it is also possible to cluster tasks into several groups, each enjoying its own feature spaces [10]. Another alternative is to resort to multilinear tensor forms that enjoy greater representational strength [15]. This approach relates to correlation analysis, which can be applied to text classification [9].

In all of the works mentioned above, it is assumed that all tasks are fully labeled. A different yet related setting of this is when some of the tasks (also called domains in some studies) are unlabeled, a setting that is often called unsupervised domain adaptation [6, 12]. Some studies consider a weakly-supervised domain adaptation problem: The problem setting is that that are multiple source domains with noisy labels in each domain; the goal is to learn a model for predicting an unlabeled target domain [25]. One idea for addressing this problem is to use curriculum learning, which trains a model from easy samples to hard samples [23]. Another work proposes to estimate the bilateral relationships between the source domain and the target domain [33]. This problem is related to the multitask weak supervision problem considered in our work, with several major distinctions. First, in our setting, the target task is fully labeled. Second, the source tasks all share the same input features. This overcomes covariate shift, a common cause of negative transfer in multitask learning. For more related works in the broader space of transfer learning, we refer interested readers to a recent survey for extensive references [32].

**Optimization methods for transfer learning.** One line of previous works to leverage cross-task information is to design optimization methods that extract information from source tasks related to the target task and discard the unrelated information. For example, one idea is to learn the task relatedness matrix for updating task weight vectors in multitask learning Saha et al. [8]. Another idea is to manipulate task gradients. Dery et al. [28] design a method that decomposes the gradients of source tasks according to the principle directions of target task gradients and keeps the gradients aligned positively with the target task. Chen et al. [29] propose a weighted training algorithm that optimizes the weights adaptively by minimizing a representation-based task distance between the source and target tasks. In this manner, the algorithm assigns higher weights to tasks more related to the target task, prioritizing relevant tasks in training.

A recent work of Chen et al. [30] uses the idea of uncertainty sampling [1] to adaptively adjust the sampling rate of each source task's data samples, thus suppressing the samples from an unrelated source task. Our task modeling approach uses a uniform sampling scheme in the source task space instead. Compared with active sampling (and reinforcement learning), uniform sampling simplifies the process of hyperparameter tuning [26]. In particular, our theoretical guarantee and computational results on the convergence of task modeling suggest that uniform sampling is a surprisingly strong approach for building task models. Combining our principled approach with uncertainty/reinforcement sampling ideas would be an interesting research question for future work.

**Pretraining and fine-tuning.** Many large self-supervised models are trained in a multitask approach over pretext tasks (e.g., masked word prediction and next sentence selection). With representations obtained with pretraining on a large amount of unlabeled, fine-tuning pretrained models is another widely used approach for transfer learning. Since fine-tuning is typically applied to target tasks with a small amount of labeled data, it is prone to over-fitting. Previous works have proposed regularization methods to constrain the distance between a fine-tuned model and the pretrained model to reduce overfitting [17, 18, 22, 27]. In particular, Our approach of modeling task relations may also benefit pretraining.

## C.2 Surrogate modeling

Our approach toward cross-task transfer learning is fundamentally different from the existing approaches in that we build on the idea of surrogate modeling [4] as a proxy of task relatedness. In particular, the use of a linear model is inspired by the findings of [31] in the context of predicting the influence of a data sample on a trained model. There is a growing body of work that uses the idea of surrogate modeling in related studies, so it is beyond the scope of this work to provide a comprehensive discussion. For example, surrogate functions can be used to approximate much more complicated model outputs, which can be used for model selection [24]. The way we estimate task models resembles Monte Carlo estimations of data Shapley [14, 16, 19, 21]. To our knowledge, these works focus on estimating the influence of a data sample. Our work instead uses surrogate modeling to estimate the influence of a task. Our findings show that this is a promising approach to model task relations. We hope our findings can inspire more studies to explore this direction and build better MTL algorithms.

### C.3 Theory of transfer learning

Compared with supervised learning, for which a systematic theoretical understanding is established [11], a theory of transfer learning has been elusive in the literature. An influential work of Baxter provides one of the earliest generalization bounds that demonstrate the benefit of learning multiple tasks within an environment of related tasks, compared with learning a single task [3]. Another early work of Ando and Zhang approaches this question from an alternating optimization perspective [5]. These statements are then refined in a later work of Maurer, Pontil, and Romera-Paredes [13].

The technical challenge for developing a theory of transfer learning is that different tasks have different data distributions. Depending on the types of distribution shift between tasks, the outcome of performing transfer learning greatly varies. A generic framework to measure distribution shift is in terms of divergences in the data distributions. For example, transfer exponent measures the difference of the density distributions between $\mathcal{P}$ and $\mathcal{Q}$ in the form of $\Pr(h \sim \mathcal{P}) \gtrsim \Pr(h \sim \mathcal{Q})^{\lambda}$, for some fixed value of $\lambda$ [20]. These works explicitly design measures to capture task relatedness. Our work offers an alternative to this problem: We show that by estimating surrogate functions of multitask predictions, one can circumvent the design of explicit task relatedness measures. Thus, the task models can be viewed as implicit measures of task relatedness. Our theoretical guarantees also show that they can capture task transfer relationships.

## References

[1] David D Lewis and Jason Catlett. “Heterogeneous uncertainty sampling for supervised learning”. In: *Machine learning proceedings 1994*. Elsevier, 1994, pp. 148–156.

[2] Sebastian Thrun and Lorien Pratt. *Learning to learn*. Springer Science & Business Media, 1998.

[3] Jonathan Baxter. “A model of inductive bias learning”. In: *Journal of artificial intelligence research* 12 (2000), pp. 149–198.

[4] Yew S Ong, Prasanth B Nair, and Andrew J Keane. “Evolutionary optimization of computationally expensive problems via surrogate modeling”. In: *AIAA journal* 41.4 (2003), pp. 687–696.

[5] Rie Kubota Ando and Tong Zhang. “A framework for learning predictive structures from multiple tasks and unlabeled data.” In: *Journal of Machine Learning Research* 6.11 (2005).

[6] Xiaojin Jerry Zhu. “Semi-supervised learning literature survey”. In: (2005).

[7] Sinno Jialin Pan, James T Kwok, Qiang Yang, et al. “Transfer learning via dimensionality reduction.” In: *AAAI*. Vol. 8. 2008, pp. 677–682.

[8] Avishek Saha, Piyush Rai, Hal Daumé III, and Suresh Venkatasubramanian. “Active online multitask learning”. In: *ICML 2010 Workshop on Budget Learning*. Citeseer. 2010.

[9] Lianghao Li, Xiaoming Jin, and Mingsheng Long. “Topic correlation analysis for cross-domain text classification”. In: *Proceedings of the AAAI Conference on Artificial Intelligence*. Vol. 26. 1. 2012, pp. 998–1004.

[10] Wenliang Zhong and James Kwok. “Convex multitask learning with flexible task clusters”. In: *ICML* (2012).

[11] Shai Shalev-Shwartz and Shai Ben-David. *Understanding machine learning: From theory to algorithms*. Cambridge university press, 2014.

[12] Mingsheng Long, Han Zhu, Jianmin Wang, and Michael I Jordan. “Unsupervised domain adaptation with residual transfer networks”. In: *Advances in neural information processing systems* 29 (2016).

[13] Andreas Maurer, Massimiliano Pontil, and Bernardino Romera-Paredes. “The benefit of multitask representation learning”. In: *Journal of Machine Learning Research* 17.81 (2016), pp. 1–32.

[14] Marco Tulio Ribeiro, Sameer Singh, and Carlos Guestrin. “" Why should i trust you?" Explaining the predictions of any classifier”. In: *KDD*. 2016, pp. 1135–1144.

[15] Mingsheng Long, Zhangjie Cao, Jianmin Wang, and Philip S Yu. “Learning multiple tasks with multilinear relationship networks”. In: *Advances in neural information processing systems* 30 (2017).

[16] Scott M Lundberg and Su-In Lee. “A unified approach to interpreting model predictions”. In: *Advances in neural information processing systems* 30 (2017).

[17] LI Xuhong, Yves Grandvalet, and Franck Davoine. “Explicit inductive bias for transfer learning with convolutional networks”. In: *International Conference on Machine Learning*. PMLR. 2018, pp. 2825–2834.

[18] Xinyang Chen, Sinan Wang, Bo Fu, Mingsheng Long, and Jianmin Wang. “Catastrophic forgetting meets negative transfer: Batch spectral shrinkage for safe transfer learning”. In: *Advances in Neural Information Processing Systems* 32 (2019).

[19] Amirata Ghorbani and James Zou. “Data shapley: Equitable valuation of data for machine learning”. In: *International Conference on Machine Learning*. PMLR. 2019, pp. 2242–2251.

[20] Steve Hanneke and Samory Kpotufe. “On the value of target data in transfer learning”. In: *NeurIPS* 32 (2019).

[21] Ruoxi Jia, David Dao, Boxin Wang, Frances Ann Hubis, Nick Hynes, Nezihe Merve Gürel, Bo Li, Ce Zhang, Dawn Song, and Costas J Spanos. "Towards efficient data valuation based on the shapley value". In: *The 22nd International Conference on Artificial Intelligence and Statistics*. PMLR. 2019, pp. 1167–1176.

[22] Xingjian Li, Haoyi Xiong, Hanchao Wang, Yuxuan Rao, Liping Liu, Zeyu Chen, and Jun Huan. "Delta: Deep learning transfer using feature map with attention for convolutional networks". In: *ICLR* (2019).

[23] Yang Shu, Zhangjie Cao, Mingsheng Long, and Jianmin Wang. "Transferable curriculum for weakly-supervised domain adaptation". In: *Proceedings of the AAAI Conference on Artificial Intelligence*. Vol. 33. 01. 2019, pp. 4951–4958.

[24] Chengrun Yang, Yuji Akimoto, Dae Won Kim, and Madeleine Udell. "OBOE: Collaborative filtering for AutoML model selection". In: *Proceedings of the 25th ACM SIGKDD international conference on knowledge discovery & data mining*. 2019, pp. 1173–1183.

[25] Yuchen Zhang, Tianle Liu, Mingsheng Long, and Michael Jordan. "Bridging theory and algorithm for domain adaptation". In: *International Conference on Machine Learning*. PMLR. 2019, pp. 7404–7413.

[26] Ekin D Cubuk, Barret Zoph, Jonathon Shlens, and Quoc V Le. "Randaugment: Practical automated data augmentation with a reduced search space". In: *Proceedings of the IEEE/CVF conference on computer vision and pattern recognition workshops*. 2020, pp. 702–703.

[27] Henry Gouk, Timothy M Hospedales, and Massimiliano Pontil. "Distance-based regularisation of deep networks for fine-tuning". In: *ICLR* (2020).

[28] Lucio M Dery, Yann Dauphin, and David Grangier. "Auxiliary task update decomposition: The good, the bad and the neutral". In: *ICLR* (2021).

[29] Shuxiao Chen, Koby Crammer, Hangfeng He, Dan Roth, and Weijie J Su. "Weighted Training for Cross-Task Learning". In: *ICLR* (2022).

[30] Yifang Chen, Kevin Jamieson, and Simon Du. "Active Multi-Task Representation Learning". In: *International Conference on Machine Learning*. PMLR. 2022, pp. 3271–3298.

[31] Andrew Ilyas, Sung Min Park, Logan Engstrom, Guillaume Leclerc, and Aleksander Madry. "Datamodels: Predicting predictions from training data". In: *ICML* (2022).

[32] Junguang Jiang, Yang Shu, Jianmin Wang, and Mingsheng Long. "Transferability in Deep Learning: A Survey". In: *arXiv preprint arXiv:2201.05867* (2022).

[33] Renchunzi Xie, Hongxin Wei, Lei Feng, and Bo An. "GearNet: Stepwise Dual Learning for Weakly Supervised Domain Adaptation". In: *AAAI* (2022).